

NASA Contractor Report 3415

NASA
CR
3415
c.1

LOAN COPY
AFWL TECH
KIRTLAND

0062279

TECH LIBRARY KAFB, NM

A Preliminary Study of Relaxation Methods for the Inviscid Conservative Gasdynamics Equations Using Flux Splitting

Joseph L. Steger

CONTRACT NAS1-15852
MARCH 1981

NASA



NASA Contractor Report 3415

A Preliminary Study of Relaxation Methods for the Inviscid Conservative Gasdynamics Equations Using Flux Splitting

Joseph L. Steger
Flow Simulations, Inc.
Sunnyvale, California

Prepared for
Langley Research Center
under Contract NAS1-15852



National Aeronautics
and Space Administration

**Scientific and Technical
Information Branch**

1981

INTRODUCTION

Time accurate and relaxation procedures for the compressible inviscid fluid conservation-law-equations (Euler equations) are frequently less efficient than procedures developed for potential flow. This is so because with the Euler equations one has to deal with a system of nonlinear partial differential equations as opposed to a single nonlinear partial differential equation in potential flow. The consequence of a system of equations is that a spectrum of associated eigenvalues must be considered so the equations are usually stiffer. Of more import, with a system of equations, the spectrum of associated eigenvalues can appear (as in subsonic flow) with both positive and negative real parts. This last restriction severely limits the choice of allowable difference operators and iterative or time dependent procedures.

The purpose of this study was to develop and test relaxation algorithms for the Euler equations which are made possible by use of flux vector similarity splittings. In this approach the flux vectors are split such that their associated Jacobian matrices have either all positive or all negative real parts. The split vectors can then be spacially differenced using dissipative forward or backward operators. A major part of the study was devoted to improving the iterative convergence rate of such relaxation algorithms, using the multi-grid approach.

BACKGROUND

A Flux Vector Split Scheme

The Euler equations can be written in conservative-vector form as

$$\partial_t \vec{q} + \partial_x \vec{E} + \partial_y \vec{F} + \partial_z \vec{G} = 0 \quad (2.1)$$

where

$$\vec{q} = \begin{bmatrix} \rho \\ \rho u \\ \rho v \\ \rho w \\ e \end{bmatrix}, \quad \vec{E} = \begin{bmatrix} \rho u \\ \rho u^2 + p \\ \rho uv \\ \rho uw \\ u(e+p) \end{bmatrix}, \text{ etc.}$$

In at least one direction we can expect a convection velocity to be less than the local sound speed. Given this condition only a restricted number of stable difference operators can be used. The problem is easily seen in one dimension if we assume subsonic flow, $u < c$ where c is the sound speed. Then

$$\partial_t \vec{q} + \partial_x \vec{E} = 0 \quad (2.2)$$

By local linearization, since $\vec{E} = \vec{E}(\vec{q})$

$$\begin{aligned} \vec{E} &= \vec{E}_0 + \left[\frac{\partial \vec{E}}{\partial \vec{q}} \right] (\vec{q} - \vec{q}_0) \\ &= \vec{E}_0 + A_0 (\vec{q} - \vec{q}_0), \quad A \text{ is the Jacobian matrix.} \end{aligned}$$

Peculiar to the Euler equations is the relation $\vec{E} = A\vec{q}$ (the equations are first degree homogeneous) so

$$\vec{E} \doteq A_0 \vec{q} \quad (2.3)$$

Thus, equation (2.2) can be locally approximated as

$$\partial_t \vec{q} + \partial_x A_0 \vec{q} = 0 \quad (2.4)$$

so that equation (2.4) becomes the linearized governing equation where A_0 is locally constant.

By similarity transform

$$A = S \Lambda S^{-1} \quad \text{or} \quad S^{-1} A S = \Lambda \quad (2.5)$$

where

$$\Lambda = \begin{bmatrix} u & 0 & 0 \\ 0 & u+c & 0 \\ 0 & 0 & u-c \end{bmatrix}$$

are the eigenvalues of A , and S has as its columns the eigenvectors of A .

Let $\vec{U} \equiv S_0^{-1} \vec{q}$, then multiply equation (2.4) by S_0^{-1} and find using equation (2.5) and freezing S_0

$$\partial_t \vec{U} + \partial_x (\Lambda_0 \vec{U})$$

or since Λ_0 is diagonal

$$\partial_t U_i + \partial_x (\lambda_i)_0 U_i \quad (2.6)$$

Because for subsonic flow $\lambda_2 = u+c > 0$ and $\lambda_3 = u-c < 0$, the operator ∂_x cannot be replaced by only a single difference operator unless that operator is a pure central difference.

All other operators will lead to exponential growth. However, first order central difference operators have problems. They tend to be nondissipative and they cannot be used with simple Euler explicit time differencing (i.e., point Jacobi relaxation). For these reasons it is difficult to devise good relaxation algorithms for the Euler equations using central differencing.

Given equation (2.6), one would have no difficulty devising stable dissipative difference operators. If $\lambda_i > 0$ let ∂_x be approximated by a backward differencing, if $\lambda_i < 0$, let ∂_x be approximated with a forward operator. Unfortunately it is impractical to try to diagonalize the Euler equations for this application. For the nonconservative equations, people have successfully differenced each term based on intuition, but this is an inappropriate way to proceed.

A rational way to split the flux terms for special differencing is based on similarity transforms and the validity of local linearization. As noted previously

$$\begin{aligned}\vec{E} &= A\vec{q} & A &\equiv \left[\frac{\partial E}{\partial q} \right] \\ &= SAS^{-1}\vec{q}\end{aligned}$$

there is no approximation here.

The plus-minus (or positive-negative) splitting is as follows:

$$\Lambda = \Lambda^+ + \Lambda^-$$

where $2\Lambda^+ = \Lambda + |\Lambda|$, that is (if $u > 0$)

$$\Lambda^+ = \begin{bmatrix} u & 0 & 0 \\ 0 & u+c & 0 \\ 0 & 0 & 0 \end{bmatrix} \quad u < c$$

$$\Lambda^+ = \begin{bmatrix} u & 0 & 0 \\ 0 & u+c & 0 \\ 0 & 0 & u-c \end{bmatrix} \quad u > c$$

and $\Lambda^- = \Lambda - \Lambda^+$.

Then

$$\begin{aligned} \vec{E} &= S\Lambda^+ S^{-1} \vec{q} + S\Lambda^- S^{-1} \vec{q} \\ &= A^+ \vec{q} + A^- \vec{q} \\ &= \vec{E}^+ + \vec{E}^- \end{aligned} \quad (2.7)$$

The flux vectors \vec{F} and \vec{G} can be split in the same way. For better clarification \vec{E}^+ is written out (2-D)

$$\vec{E}^+ = (\rho/\gamma) \begin{bmatrix} (\gamma-1)\lambda_1^+ + .5(\lambda_3^+ + \lambda_4^+) \\ (\gamma-1)u\lambda_1^+ + .5u(\lambda_3^+ + \lambda_4^+) + .5c(\lambda_3^+ - \lambda_4^+) \\ (\gamma-1)v\lambda_1^+ + .5v(\lambda_3^+ + \lambda_4^+) \\ .5(\gamma-1)(u^2+v^2)\lambda_1^+ + .25(u^2+v^2+2cu+2c^2/(\gamma-1))\lambda_3^+ \\ \quad + .25(u^2+v^2 - 2cu + 2c^2/(\gamma-1))\lambda_4^+ \end{bmatrix} \quad (2.8)$$

$$\lambda_1^+ = \frac{u+|u|}{2}, \quad \lambda_3^+ = \frac{(u+c)+|u+c|}{2}, \quad \lambda_4^+ = \frac{(u-c)+|u-c|}{2}$$

The vector E^- is obtained by replacing λ^+ by λ^- , while F^+ and F^- use $\lambda_1^\pm = (v \pm |v|)/2$, etc.

The advantage of the new splitting is that the eigenvalues associated with the Jacobian of E^+ are always positive while those of E^- are always negative. Consequently for the Euler equations split as

$$\partial_t \vec{q} + \partial_x (\vec{E}^+ + \vec{E}^-) + \partial_y (\vec{F}^+ + \vec{F}^-) + \partial_z (\vec{G}^+ + \vec{G}^-) = 0 \quad (2.9)$$

one can easily pick stable dissipative spatial difference operators. For example, a stable point Jacobi relaxation scheme is given by

$$\begin{aligned} \vec{q}^{n+1} = \vec{q}^n - \omega (\delta_x^B \vec{E}^+ + \delta_y^B \vec{F}^+ + \delta_z^B \vec{G}^+ + \\ + \delta_x^F \vec{E}^- + \delta_y^F \vec{F}^- + \delta_z^F \vec{G}^-)^n \end{aligned} \quad (2.10)$$

where

$$\begin{aligned} \delta_x^B u_j &= (3u_j - 4u_{j-1} + u_{j-2}) / (2\Delta x^2) & O(\Delta x^2) \\ \delta_x^F u_j &= (-3u_j + 4u_{j+1} - u_{j+2}) / (2\Delta x^2) & O(\Delta x^2) \\ & \text{etc.} \end{aligned} \quad (2.11)$$

A stable, easily inverted implicit scheme is given by

$$\begin{aligned} [I + h(\delta_x^B A + \delta_y^B B^+ + \delta_z^B C^+)] [I + h(\delta_x^F A^- + \delta_y^F B^- \\ + \delta_z^F C^-)] (\vec{q}^{n+1} - \vec{q}^n) = -h(\delta_x^B \vec{E}^+ + \delta_y^B \vec{F}^+ \\ + \delta_z^B \vec{G}^+ + \delta_x^F \vec{E}^- + \delta_y^F \vec{F}^- + \delta_z^F \vec{G}^-)^n \end{aligned} \quad (2.12)$$

The implicit algorithm was a chief motivation for + and - splitting. The left hand side is factored into pure block lower and pure block upper triangular matrices and these are trivial to invert by simple sweeps (like SOR). Compared to inverting block tridiagonal matrices in x, y, and z, the + and - inversion cost is very small. The differencing also does not require artificial viscosity. The disadvantages of the + and - implicit scheme are that twice as many Jacobian matrices have to be formed (although A, B, and C can be formed all together making up some of the loss), and no satisfactory way has been devised to time accurately treat viscous terms in upper and lower implicit factorizations.

A more thorough discussion of the "upwind" flux vector split scheme is given in reference [1] along with a review of previous related work. Additional new work in this area is given in references [2] through [6].

As an aside, it is noted that the fact that the Euler equations are homogeneous of degree one has been used in formulating the splitting scheme. For systems of conservation laws in which the flux vectors are not homogeneous, one can still proceed as before if one solves for a delta variable. Consider, for example, the system

$$\partial_t u + \partial_x f + \partial_y g = 0 \quad (2.13)$$

where $f = f(u)$, $g = g(u)$, but $\frac{\partial f}{\partial u} u \neq f$ and $\frac{\partial g}{\partial u} u \neq g$.

Let u_0 be a nearby solution of equation (2.13), then expanding u, f, and g about u_0 ,

$$\begin{aligned} \partial_t [u_0 + I(u-u_0)] + \partial_x [f_0 + A_0(u-u_0)] \\ + \partial_y [g_0 + B_0(u-u_0)] = 0 + 0(u-u_0)^2 \end{aligned} \quad (2.14)$$

where $A \equiv \frac{\partial f}{\partial u}$, $B \equiv \frac{\partial g}{\partial u}$. Then as u_0 satisfies (2.13), equation (2.14) is rewritten as

$$\partial_t U + \partial_x A_0 U + \partial_y B_0 U = 0 \quad (2.15a)$$

and

$$U = u - u_0 \quad (2.15b)$$

Equation (2.15) can now be split as were the Euler equations with $A = A^+ + A^-$ and $B = B^+ + B^-$ assuming that A and B can both be diagonalized. Note that because $U = u - u_0$ is the new dependent variable, the scheme (2.15) will only be first order accurate in time if A_0 is set to A^n and U is set to $u^{n+1} - u^n$. If A_0 is set to A^{n+1} and U is set to $(3u^{n+1} - 4u^n + u^{n-1})/2$, second order accuracy can result. For steady state problems one can use $u - u_0 = u_j - u_{j-1}$, etc. if, for example, u_j is known at $j = 1$ and u_1 satisfies the steady form of (2.13). This technique has not been tested in steady cases.

It is stressed that no computational experience has been gained with split forms of equation (2.15). While + and - split forms of equation (2.15) are not as computationally efficient as (2.9), they apparently will not suffer from the annoyance that $\frac{\partial E^+}{\partial q} \neq A^+$ etc. as discussed in Ref. 1.

Multigrid

A major emphasis of this study was to apply the multigrid relaxation methodology [7] - [10] to the flux vector split form of the differenced Euler equations. The multigrid procedure has been notably successful in treating elliptic second order partial differential equations, and recently has been applied to the transonic potential equations [9], [11], [12]. Considerably less experience is available with first order systems of partial differential equations.

The multigrid method has been described in various publications, and it is clear from these papers that the method is still in a state of change. The work of Brandtl, who is perhaps multigrid's most distinguished proponent, treats multigrid as a smoothing process in which coarse grids are used to damp low frequency components of a solution and fine grids are used to damp high frequency content. A recent paper by Jameson [11] used multigrid with an alternating direction algorithm in which the various grids effectively supply a sequence of relaxation parameters to damp the spectrum of frequencies associated with a given solution. In another recent work McCormick [13] has analysed multigrid procedures as a means of supplying efficient conditioning matrices to a relaxation procedure. The concept of high and low frequency content is again observed in this analysis.

With the exception of some very simple model problems, the multigrid procedure is too complex to treat by analysis. (The analysis should account for the interpolation process, boundary conditions, and so on.) Consequently, one must proceed using simplified analysis and trial and error. The danger here is that it may be difficult to identify the crucial elements of a successful multigrid procedure.

The multigrid procedure used in the current work is essentially that which has been referred to as the full approximation. [9] The general forms used are described below. However, there are various strategies for sequencing through and interpolating from grid level to grid level. These have not been faithfully followed in the results to be presented later.

Let $G_1, G_2, G_3, \dots, G_m, \dots, G_M$ be grids with ever increasing finess such that G_2 is half the spacing of G_1 , G_3 is half the spacing of G_2 , etc. Using multigrid sweeps the variables are updated on the m th grid as

$$Q_m^{n+1} = Q_m^n + H_m [R_m(Q^n) - R_m(\tilde{q}) + I_M^m R_M(\tilde{q})] \quad (2.16)$$

where the residuals are used directly rather than their local linearizations.

$$R_m(Q^n) = A_m Q_m^n - f_m$$

$$R_m(\tilde{q}) = A_m \tilde{q} - f_m$$

Here q represents the best fine grid (i.e., G_M) estimate of the exact difference equation solution

$$R_M(q) = 0 = \delta_x^b E^+ + \delta_y^f E^- + \delta_y^b F^+ + \delta_y^f F^-$$

The variable Q_m is the update variable. At the end of each multigrid sweep \tilde{q} is replaced by Q_M , while in changing from grid to grid the discrepancy is updated:

$$Q_{m+1} = I_M^{m+1} \tilde{q} + I_m^{m+1} (Q_m - I_M^m \tilde{q}).$$

The matrix H is a conditioning matrix which is formed as part of the chosen relaxation scheme, while A_m is the Jacobian matrix, $\frac{\partial R}{\partial q}$. The operator I_m^{m+1} means to interpolate data from coarse grid m to finer grid $m+1$. The operator I_m^{m-1} means to average (or inject) data from fine grid m to coarser grid $m-1$.

As an alternate to equation (2.16), the update formula

$$Q_m^{n+1} = Q_m^n + H_m [A_m(\tilde{q})Q_m^n - A_m(\tilde{q})\tilde{q} + I_M^m R_M(\tilde{q})] \quad (2.17)$$

has also been used. This last form, which is more costly to form, has the nonlinearity frozen over a multigrid sweep.

The multigrid procedures defined above essentially duplicate the full approximation scheme of South and Brandt. Motivation for the various steps in this procedure can be found in reference [9] or in Appendix A. In Appendix A, the basic steps of the multigrid process are derived using simple expansion and interpolation ideas.

ONE-DIMENSIONAL FLOW STUDY

Numerical Schemes

If one is careful to avoid direct-inversion fully implicit schemes, it is possible to test relaxation algorithms for the Euler equations in one dimension. The one dimensional nozzle flow equations are given by

$$\partial_{\mathbf{x}} \hat{\mathbf{F}} + \hat{\mathbf{H}} = 0 \quad (3.1)$$

where

$$\hat{\mathbf{q}} = A \begin{bmatrix} \rho \\ \rho u \\ e \end{bmatrix}, \quad \hat{\mathbf{F}} = A \begin{bmatrix} \rho u \\ \rho u^2 + p \\ u(e+p) \end{bmatrix}, \quad \hat{\mathbf{H}} = -p \begin{bmatrix} 0 \\ A_{\mathbf{x}} \\ 0 \end{bmatrix} \quad (3.2)$$

Here A is the area ratio and $A_{\mathbf{x}}$ is $\frac{\partial A}{\partial x}$. In one dimension, pressure is related to the other variables via

$$p = (\gamma - 1)(e - \frac{1}{2}\rho u^2) \quad (3.3)$$

Using flux vector splitting, (3.1) is differenced as

$$\delta_{\mathbf{x}}^b \hat{\mathbf{F}}^+ + \delta_{\mathbf{x}}^f \hat{\mathbf{F}}^- + \hat{\mathbf{H}} = 0 = R(\mathbf{q}) \quad (3.4)$$

where

$$F^{\pm} = \frac{\rho A}{2\gamma} \begin{bmatrix} 2(\gamma-1) \lambda_1^{\pm} + \lambda_2^{\pm} + \lambda_3^{\pm} \\ 2(\gamma-1)u\lambda_1^{\pm} + \lambda_2^{\pm}(u+c) + \lambda_3^{\pm}(u-c) \\ (\gamma-1)\lambda_1^{\pm} u^2 + \frac{\lambda_2^{\pm}(u+c)^2}{2} + \frac{\lambda_3^{\pm}(u-c)^2}{2} + W \end{bmatrix} \quad (3.5)$$

$$\text{where } W = \frac{(3-\gamma)(\lambda_2^+ + \lambda_3^+)c^2}{2(\gamma-1)}$$

$$\lambda_1^{\pm} = \frac{u \pm |u|}{2} \quad \text{etc.} \quad (3.6)$$

and

$$\begin{aligned}\delta_x^b F &= \frac{3F_j - 4F_{j-1} + F_{j-2}}{2\Delta x} \\ \delta_x^f F &= \frac{-3F_j + 4F_{j+1} - F_{j+2}}{2\Delta x}\end{aligned}\quad (3.7)$$

Two iterative schemes have been tested for equation (3.4).

The first is point Jacobi

$$\hat{q}_j^{n+1} = \hat{q}_j^n - \omega \left(\frac{2\Delta x}{3} \right) \left(\frac{\partial F^+}{\partial q} - \frac{\partial F^-}{\partial q} \right)^{-1} R_j^n \quad (3.8)$$

where $\frac{\partial F^+}{\partial q}$ and $\frac{\partial F^-}{\partial q}$ are the Jacobian matrices and \hat{q} is defined in (3.2). The second is an approximate factorization (AF) scheme

$$\begin{aligned}(\mathbf{I} + \omega \delta_x^b \frac{\partial F^+}{\partial q})(\mathbf{I} + \omega \delta_x^f \frac{F^-}{q})(\hat{q}^{n+1} - \hat{q}^n) \\ = - \omega R_j^n\end{aligned}\quad (3.9)$$

Note that the second scheme could be solved without approximate factorization in the block pentadiagonal form

$$(\mathbf{I} + \omega \delta_x^b \frac{\partial F^+}{\partial q} + \omega \delta_x^f \frac{\partial F^-}{\partial q})(\hat{q}^{n+1} - \hat{q}^n) = - \omega R_j^n \quad (3.10)$$

with $\omega \gg 1$. Such a process cannot be efficiently repeated in multidimensional, however, so only the factored form (3.9) is considered. The form (3.9) is representative of multi-dimensions since essentially the same type of lower and upper factored forms are obtained in two or three dimensions.

For comparison purposes a centrally differenced form of (3.1) was also considered. In this case the flux vector \hat{F} was split into a convection term and a pressure or sound speed term, i.e.

$$\hat{F} = \hat{F}_u + \hat{F}_c \quad (3.11)$$

with $\hat{F}_u = u\hat{q}$ and $\hat{F}_c = \hat{F} - \hat{F}_u$. This splitting was arbitrarily introduced for the purpose explained below. Introducing (3.11) into (3.1) and central differencing gives

$$\delta_x \hat{F}_u + \delta_x \hat{F}_c + \hat{H} = 0 = R_c(q) \quad (3.12)$$

where

$$\delta_x F = \frac{F_{j+1} - F_{j-1}}{2\Delta x}$$

This set of difference equations was then solved via the implicit approximately factored scheme

$$\begin{aligned} & \left[I + \omega \delta_x A_u^n + (\epsilon + h^2 + |\nabla \Delta q^n|) \nabla \Delta \right] \left[I + \omega \delta_x A_c^n \right. \\ & \quad \left. + (\epsilon + h^2 + |\nabla \Delta q^n|) \nabla \Delta \right] (q_j^{n+1} - q_j^n) \\ & = -\omega R_c(q^n) + (\epsilon \nabla \Delta + h^2 + |\nabla \Delta q^n|) \nabla \Delta q_j^n \end{aligned} \quad (3.13)$$

where

$$A_u = \begin{bmatrix} 0 & 1 & 0 \\ -u^2 & 2u & 0 \\ ue/\rho & e/\rho & u \end{bmatrix} \quad \text{or} \quad A_u = \begin{bmatrix} u & 0 & 0 \\ 0 & u & 0 \\ 0 & 0 & u \end{bmatrix} \quad (3.14a)$$

$$A_c = (\gamma-1) \begin{bmatrix} 0 & 0 & 0 \\ u^2/2 & -u & 1 \\ (u^3 - ue/\rho) & (e/\rho - \frac{3}{2} u^2) & u \end{bmatrix} \quad (3.14b)$$

and numerical dissipation terms are added to the equations with $h \sim \Delta x$, $\varepsilon = 0(.06)$, and $\nabla q_j = q_j - q_{j-1}$, etc. This way of treating the dissipation terms was developed over several years, but see also Appendix B.

Note that equation (3.12) could have been written as one factor and then easily inverted via a block tridiagonal solver. With $\omega \rightarrow \infty$ this amounts to a direct inversion of the linearized equations. The splitting equation (3.11) allows use of the approximately factored form, equation (3.13) which is the type of factorization required in multi-dimensions. Thus, it is suspected that information learned from study of the scheme equation (3.13) will apply to the multi-dimensional case. One other point--the matrices A_u and A_c are not the Jacobians $\frac{\partial F_u}{\partial q}$ and $\frac{\partial F_c}{\partial q}$, because use of the Jacobians leads to numerical instability. However, the matrices A_u and A_c , developed in reference [14] via similarity to $\frac{\partial F}{\partial q}$, are stable. It is remarked that the eigenvalues of $\frac{\partial F_u}{\partial q}$ are u, u, u , those of $\frac{\partial F_c}{\partial q}$ are $0, \pm \sqrt{\frac{\gamma-1}{\gamma}} c$. The eigenvalues of A_u are u, u, u , while those of A_c are $0, c, -c$.

One Dimensional Results

One dimensional nozzle flow was selected as a test. The nozzle was chosen with area ratio

$$A = 1 - .8 x (1-x) \quad 0 \leq x \leq 1$$

which has a throat to exit ratio of 0.8. The entrance area ratio at $x = 0$ is equal to the exit area ratio at $x = 1$. The incoming Mach number must reach a value of 0.55332 for the throat to reach sonic conditions. In all one dimensional test cases, boundary data at both entrance and exit is fully specified. This overspecification of boundary data is expected to aid the iterative rate of convergence.

Subsonic flow convergence rates for plus and minus flux vector split schemes, equations (3.8) and (3.9), are indicated in figure (3.1). Here the maximum residual is plotted as a function of fine grid iteration number. The ℓ_2 norm of the residuals was also monitored, and this showed a similar, although somewhat more monotone, trend. A sixty five point grid was used. On this grid the subsonic flow results are indistinguishable from the exact solution on a typical plot.

It was hoped that the multigrid scheme would make even the point Jacobi scheme converge quickly. As indicated in figure (3.1) this was not the case. Of course, some modification of the current multigrid scheme may lead to a quite different result. In this and all of the one dimensional calculations the multigrid scheme (2.16) was used.

The point Jacobi scheme was quickly dropped as it requires as much computational work per step as the AF scheme, equation (3.9). The AF scheme converges well by itself. With use of multigrid, however, the rate of convergence is improved by a factor of 4, (see figure (3.1)). Of course, the multigrid scheme requires more work per point, but this result is promising. It is noted that in the multigrid approach that sweeps from coarsest grid to finest grid proved more efficient than sweeping down from the finest

grid and then back up from the coarsest to the finest grid. Linear interpolation was used to go from a coarse to a fine grid. Injection (not averaging) was used to go from a fine to a coarse grid. By injection is meant that the fine grid result is used on the coarse grid, as the coarse grid points occupy the same position as the fine grid points.

Numerical results for supercritical shocked flow are indicated in figure (3.2) versus the exact solution. The small "glitch" at the sonic line is due to a discontinuous change of the λ^+ and λ^- eigenvalues. This effect would be more pronounced, but smoothing has been added by simply replacing λ^\pm by

$$\bar{\lambda}^\pm = \lambda^\pm \pm \epsilon$$

where ϵ is small. This effectively adds

$$\epsilon(\delta_x^b - \delta_x^f)\hat{q} = \epsilon(\Delta x)^3 \delta_{xxxx} \hat{q}$$

to the equations, where δ_{xxxx} is the five point centered difference approximation to the fourth derivative.

The rate of convergence for the AF scheme with and without multigrid acceleration is indicated by figure (3.3). Again a sixty five point grid is used. While the multigrid scheme ends with a much faster rate of convergence, it does not reach a converged state any faster than the standard algorithm.

The central differencing scheme was also run for this flow. Numerical results are shown in figure (3.4), while the convergence rate is indicated via figure (3.5). Here the multigrid procedure gives a superior rate of convergence to the conventional scheme, and overall, it nearly matches the rate achieved with plus and minus flux vector splitting.

The use of the dissipation terms are crucial to the success of this method. While this way of treating the dissipation terms was derived over some years, their treatment is motivated from the plus and minus flux vector split terms as indicated in Appendix B.

TWO DIMENSIONAL FLOW STUDY

Test Problem and Numerical Scheme

As a test problem in two dimensions, the flow about a nonlifting biconvex airfoil was used. Thin airfoil boundary conditions were specified so as to simplify the imposition of the tangency condition. As a result it was unnecessary to introduce transformations to fit the body surface. However, simple clustering transformations of the form

$$\begin{aligned}\xi &= \xi(x) \\ \eta &= \eta(y)\end{aligned}\tag{4.1}$$

were used so as to stretch the far field boundaries far from the airfoil. The transforms also provide good grid resolution near the body, especially at the leading and trailing edges of the biconvex profile.

With introduction of the ξ, η variables the governing equations take on the form

$$\partial_{\xi} y_{\eta} (E^{+} + E^{-}) + \partial_{\eta} x_{\xi} (F^{+} + F^{-}) = 0\tag{4.2}$$

where E^{\pm} was given by equation (2.8) and F^{\pm} are similar (see reference [1] to obtain the actual elements). Note that E and F remain the original Cartesian form of the flux vectors, only the independent variables are transformed.

A multigrid relaxation algorithm is developed for equation (4.2) using the approximate factorization scheme (2.9) and the full approximation multigrid method (2.17). The precise algorithm used is

$$\begin{aligned}
& [I + \bar{h}_m (\delta_{\xi}^B y_{\eta} A^+ + \delta_{\eta}^B x_{\xi} B^+)] [I + \bar{h}_m (\delta_{\xi}^F y_{\eta} A^- + \delta_{\eta}^F x_{\xi} B^-)] (Q_m^{n+1} - Q_m^n) \\
& = - \bar{h}_m R_m
\end{aligned} \tag{4.3}$$

where

$$\begin{aligned}
R_m = & (\delta_{\xi}^B y_{\eta} A^+ + \delta_{\eta}^B x_{\xi} B^+ + \delta_{\xi}^F y_{\eta} A^- + \delta_{\eta}^F x_{\xi} B^-)_m (Q^n - I_M^m \tilde{q}) \\
& + I_M^m (\delta_{\xi}^B y_{\eta} E^+ + \delta_{\eta}^B y_{\eta} F^+ + \delta_{\xi}^F x_{\xi} E^- + \delta_{\eta}^F x_{\xi} F^-)
\end{aligned}$$

and A^+ , B^+ , E^+ , etc. are evaluated using \tilde{q} .

The parameter \bar{h}_m is a relaxation parameter which varies from point to point as

$$\tilde{h}_m = J h_m, \quad h_m = \frac{0(0.2)}{m} \tag{4.4}$$

A more conventional scaling would use

$$\tilde{h}_m = h_m / (y_{\eta} + x_{\xi}) \quad h_m = 0(?) \tag{4.5}$$

and perhaps (4.5) or alternation of (4.4) with (4.5) would be preferred to (4.4).

All of the far field boundary conditions for the nonlifting biconvex airfoil are set to free stream values. A stretched grid is used and these boundaries are placed 3 chord lengths in front of and behind the airfoil. The upper boundary $y = y_{\max}$ is set at 8 chords away from the $y = 0$ plane. Along the $y = 0$ line the vertical velocity v is obtained via

$$v = U_{\infty} \frac{dy}{dx} \tag{4.6}$$

where $\frac{dy}{dx} = 2\tau(1-x)$, $0 \leq x \leq 1$, and $\frac{dy}{dx} = 0$ elsewhere. All other variables along $y = 0$ are obtained from $\frac{\partial q}{\partial y} = 0$. In the multigrid scheme this implies that

$$(Q_m - I_M^m \tilde{q})_{j,1} = (Q_m - I_M^m \tilde{q})_{j,2} \quad (4.7)$$

Results

Subsonic flow results about a six percent thick parabolic arc airfoil are shown in figure 4.1. The Mach number is 0.817. These results, which use the thin airfoil boundary condition, are comparable to those obtained in potential schemes. The numerical solution shows slight asymmetry about the midchord and this may be taken as a measure of error in the solution. A stretched grid with 65 points in x and 33 points in y is used.

Convergence rates for this case without using multigrid acceleration are indicated in figure 4.2 for various values of h_m . The best multigrid results obtained to date are indicated in figure 4.3. The multigrid procedure is perhaps four times faster and gives a fully converged solution in less than 50 fine grid iterations. It is remarked that linear interpolation and injection (not averaging) is used in the multigrid procedure. It is also noted that the grid spacing does vary rapidly. In particular, $\Delta x_{\max}/\Delta x_{\min} = 36.06$ and $\Delta y_{\max}/\Delta y_{\min} = 44.2$ so grid aspect ratios are of $O(40)$.

Supercritical flow results about a 12% thick profile are shown in figure 4.4 for various smoothing ratios, i.e.

$$\lambda^{\pm} = \frac{\lambda \pm |\lambda|}{2} \pm \epsilon, \quad \epsilon \text{ a constant}$$

Here the Mach number is 0.8.

Convergence rates obtained without using multigrid are given in figure 4.5, the best multigrid results appear in figure 4.6. The multigrid result appears to be about twice as fast as the nonmultigrid result and it requires about 120 fine grid iterations using the grid of 65×33 . Perhaps the multigrid procedure is less effective for transonic flow because of the extensive discontinuous switching that occurs in the split flux vector formulation.

CONTINUOUS DERIVATIVE PLUS-MINUS SPLIT FLUX VECTORS

As the results in both one and two dimensions illustrate, small "glitches" appear at the sonic line when the plus-minus flux vector splitting is used. This is because the flux vectors depend on the $|\lambda|$, as indicated via equation (2.8) or (3.6). As λ changes sign, $|\lambda|$ has a discontinuous first derivative. Consequently, the flux vectors also have a discontinuous first derivative when any eigenvalue changes sign. This occurs at the sonic line and causes numerical inaccuracy there, a glitch.

In reference [1] it was noted that the λ^\pm should be redefined as

$$\lambda^\pm = \frac{\lambda \pm |\lambda|}{2} \pm \beta, \quad \beta \text{ positive} \quad (5.1)$$

where " β is a small positive number which smoothly approaches zero as $|\lambda|$ increases." In this way λ^\pm could be kept smooth, however, no simple formula for β was proposed.

The appearance of discontinuous first derivatives in the definition of the flux vectors prompted van Leer of ICASE to postulate new flux vectors. In one dimension he proposed (unpublished)

$$(u - c) < 0$$

$$F^+ = \begin{bmatrix} f_{1+}^+ \\ f_{2+} \\ f_3 \end{bmatrix} = \begin{bmatrix} \rho c (M+1)^2 / 4 \\ \rho c^2 (M+1)^2 [(\gamma-1)M+2] / [4\gamma] \\ \gamma^2 [(f_2^+)^2 / f_1^+] / [2(\gamma^2-1)] \end{bmatrix} \quad (5.2a)$$

$$F^- = F - F^+ \quad (5.2b)$$

and

$$u - c > 0 \quad F^+ = F, \quad F^- = 0 \quad (5.3)$$

Here

$$F = \begin{bmatrix} \rho c M \\ \rho c^2 (M^2 + \gamma^{-1}) \\ \rho c^3 [(M^2/2) + (\gamma-1)^{-1}] M \end{bmatrix} = \begin{bmatrix} \rho u \\ \rho u^2 + p \\ u(e + p) \end{bmatrix} \quad (5.4)$$

These vectors have functional variation much like those proposed by Steger and Warming [1]. However, they have a continuous first derivatives at $u = c$ and at $u = 0$. Analysis by van Leer verifies their stability as do our own numerical tests. On the nozzle problem the van Leer vectors give the excellent steady state result shown in figure (5.2) which has a smooth transition across the sonic line. The second order upwind spacial difference operators, (3.7), were used.

The success of van Leer's scheme prompted another search for a clean way to define β in equation (5.1). This was ultimately achieved by simply replacing the $|\lambda|$ with $\sqrt{\lambda^2 + \epsilon^2}$. As shown in figure (5.1), this amounts to fitting a hyperbola to the $|\lambda|$ versus λ curve.

Thus λ^\pm are redefined as

$$\lambda^\pm = \frac{\lambda \pm \sqrt{\lambda^2 + \epsilon^2}}{2} \quad (5.5)$$

and β of equation (5.1) is indeed positive and equal to

$$\beta = \frac{\sqrt{\lambda^2 + \varepsilon^2} - |\lambda|}{2} \quad (5.6)$$

Use of (5.5) to define λ^\pm also leads to split plus minus flux vectors with continuous derivatives. One dimensional nozzle flow results using this definition of λ are indicated in figure (5.3). Here the variation at the sonic line is smooth, while compared to the previous result figure (3.2), the shock solution is essentially unchanged.

CONCLUDING REMARKS

Relaxation algorithms were devised for the steady gas dynamic equations in conservation-law-form using flux vector splitting and the multigrid technique. Overall, fairly good steady state convergence rates were obtained although the multigrid method was not made as effective as what appears to be possible. Considerable additional work remains to be undertaken.

In closing it is noted that other promising approaches for relaxing the Euler equations are beginning to appear. These include the surrogate equation approach of Johnson [15]. As a final digression it is suggested that a time-accurate second degree wave equation formulation, as detailed in Appendix C, might offer another entertaining approach.

REFERENCES

1. Steger, J. L. and Warming, R. F., Flux Vector Splitting of the Inviscid Gasdynamic Equations with Application to Finite Difference Methods. NASA TM 78605, 1979.
2. Chakravarthy, S. R., Anderson, D. A., and Salas, M. D., The Split Coefficient Matrix Method for Hyperbolic Systems of Gas-Dynamic Equations. AIAA Paper 80-0268, Pasadena, California, 1980.
3. Sells, C. C. L., Numerical Solutions of the Euler Equations for Steady Transonic Flow Past a Lifting Aerofoil. GAMM Workshop Proceedings, Stockholm, Sweden, 1979.
4. Osher, S., Numerical Solution of Singular Perturbation Problems and Hyperbolic Systems of Conservation Laws. Research notes prepared under NASA Ames University Consortium, 1980.
5. Roe, P. J., The Use of the Riemann Problem in Finite Difference Schemes. Paper presented at the Seventh International Conference on Numerical Methods in Fluid Dynamics, Stanford, California, 1980.
6. Pandolfi, M. and Zannetti, L., A Physical Approach to Solve Numerically Complicated Hyperbolic Flow Problems. Paper presented at the Seventh International Conference on Numerical Methods in Fluid Dynamics, Stanford, California, 1980.
7. Brandt, Achi, Multi-Level Adaptive Technique (MLAT) for Fast Numerical Solution of Boundary Value Problems. Proceedings of the Third International Conference on Numerical Methods in Fluid Mechanics, 1972.
8. Brandt, A., Multi-Level Adaptive Solutions to Boundary-Value Problems. ICASE Report 76-27, 1976.
9. South, J. and Brandt, A., Application of a Multi-Level Grid Method to Transonic Flow Calculations. ICASE Report 76-8, 1976.

10. Brandt, A., Multi-Level Adaptive Computations in Fluid Dynamics. AIAA Paper No. 79-1455, Proceeding AIAA Computational Fluid Dynamics Conference, Williamsburg, Virginia, 1979.
11. Jameson, A., Acceleration of Transonic Potential Flow Calculations on Arbitrary Meshes by the Multiple Grid Method. AIAA Paper No. 79-1458, Proceeding AIAA Computational Fluid Dynamics Conference, Williamsburg, Virginia, 1979.
12. McCarthy, D. R. and Reyhner, T. A., A Multi-Grid Code for Three-Dimensional Transonic Potential Flow About Axisymmetric Inlets at Angle of Attack. AIAA Paper No. 80-1365, 1980.
13. McCormick, S. F., Multigrid Methods: Alternate Viewpoint. Lawrence Livermore Laboratory Report, UCID-18487, 1979.
14. Steger, J. L., Coefficient Matrices for Implicit Finite Difference Solution of the Inviscid Fluid Conservation Law Equations. Computer Methods in Applied Mechanics and Engineering 13 (1978), p. 175.
15. Johnson, G. M., An Alternative Approach to the Numerical Simulation of Steady Inviscid Flow. NASA TM-81542, Presented at the Seventh International Conference of Numerical Methods in Fluid Dynamics, Stanford, CA, 1980.

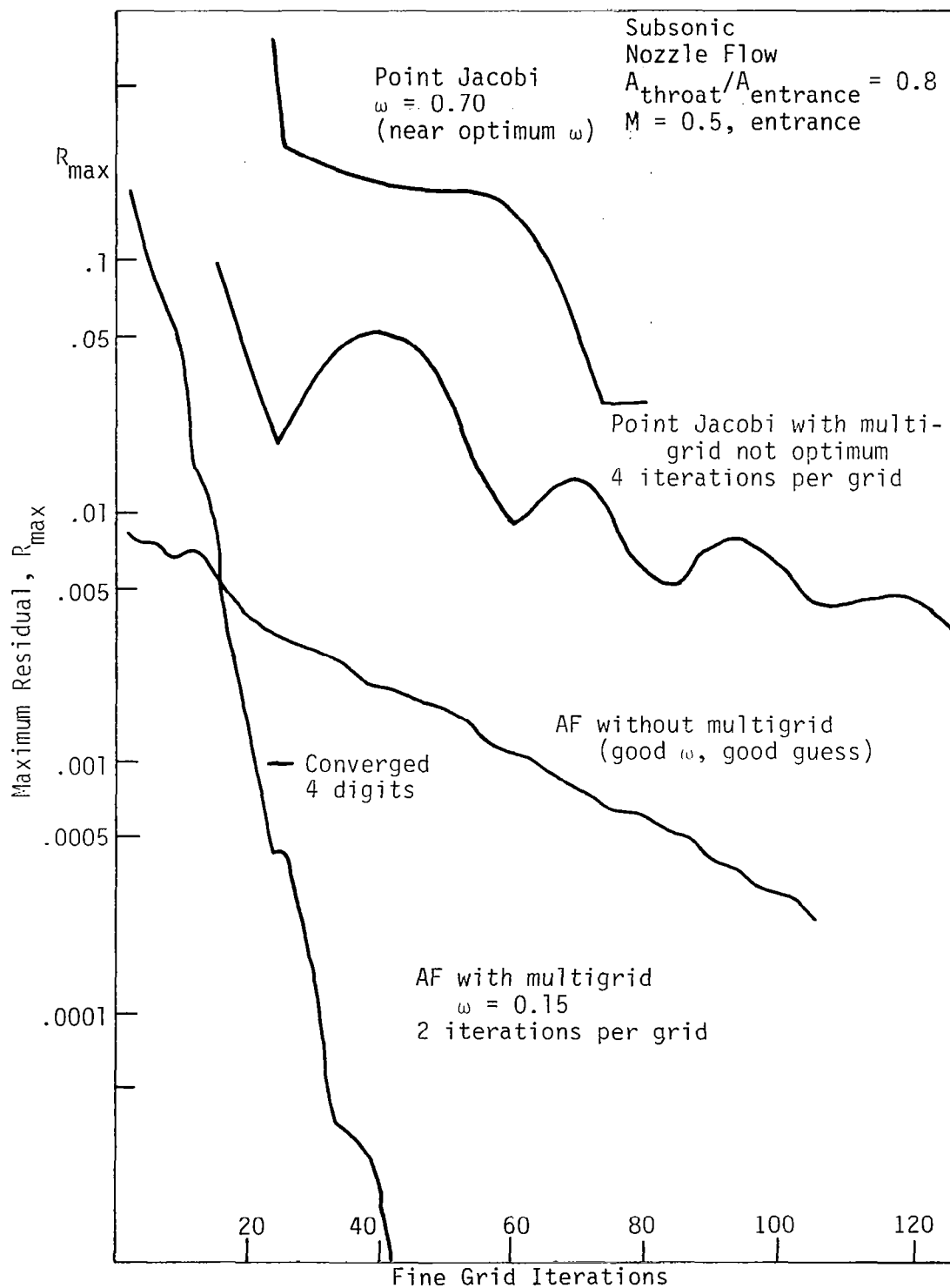


Fig. 3.1. Convergence history.

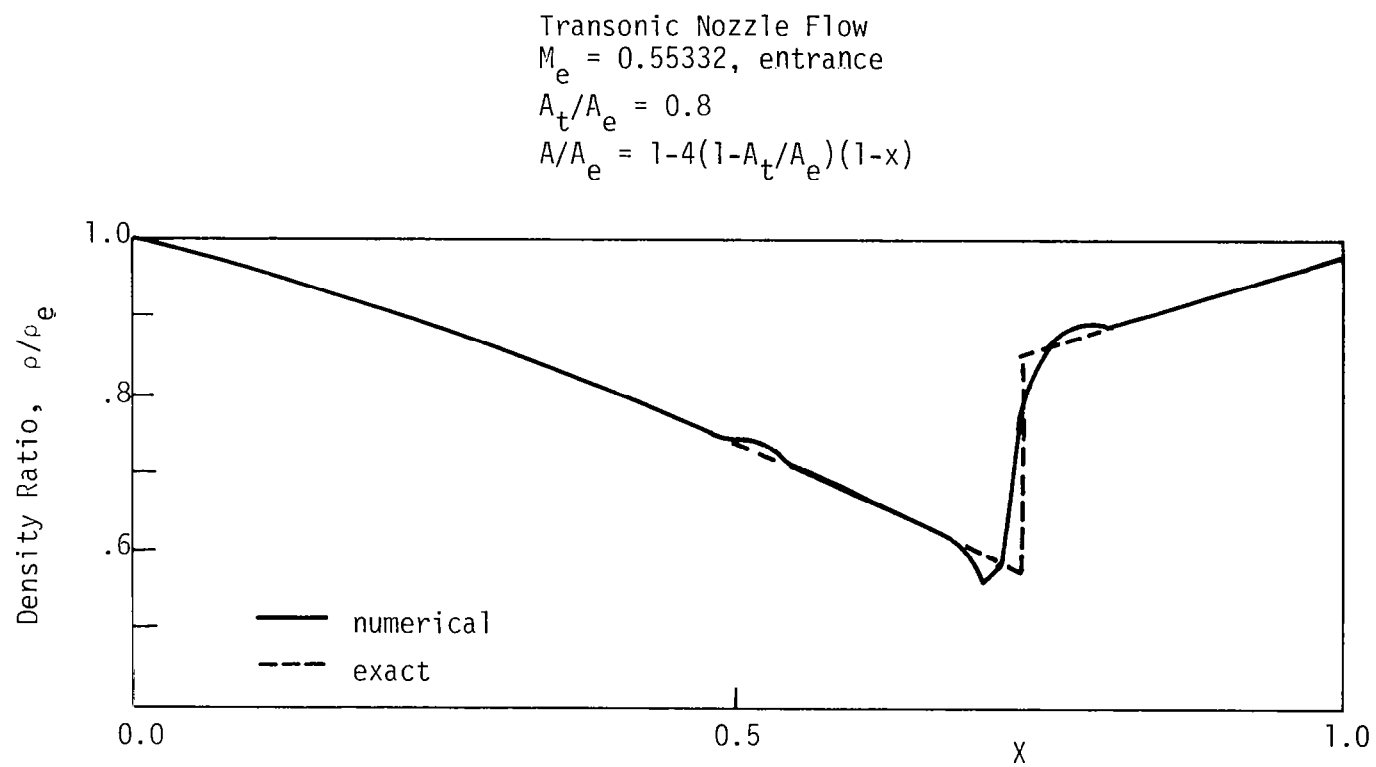


Fig. 3.2. Solution from plus-minus flux split algorithm.

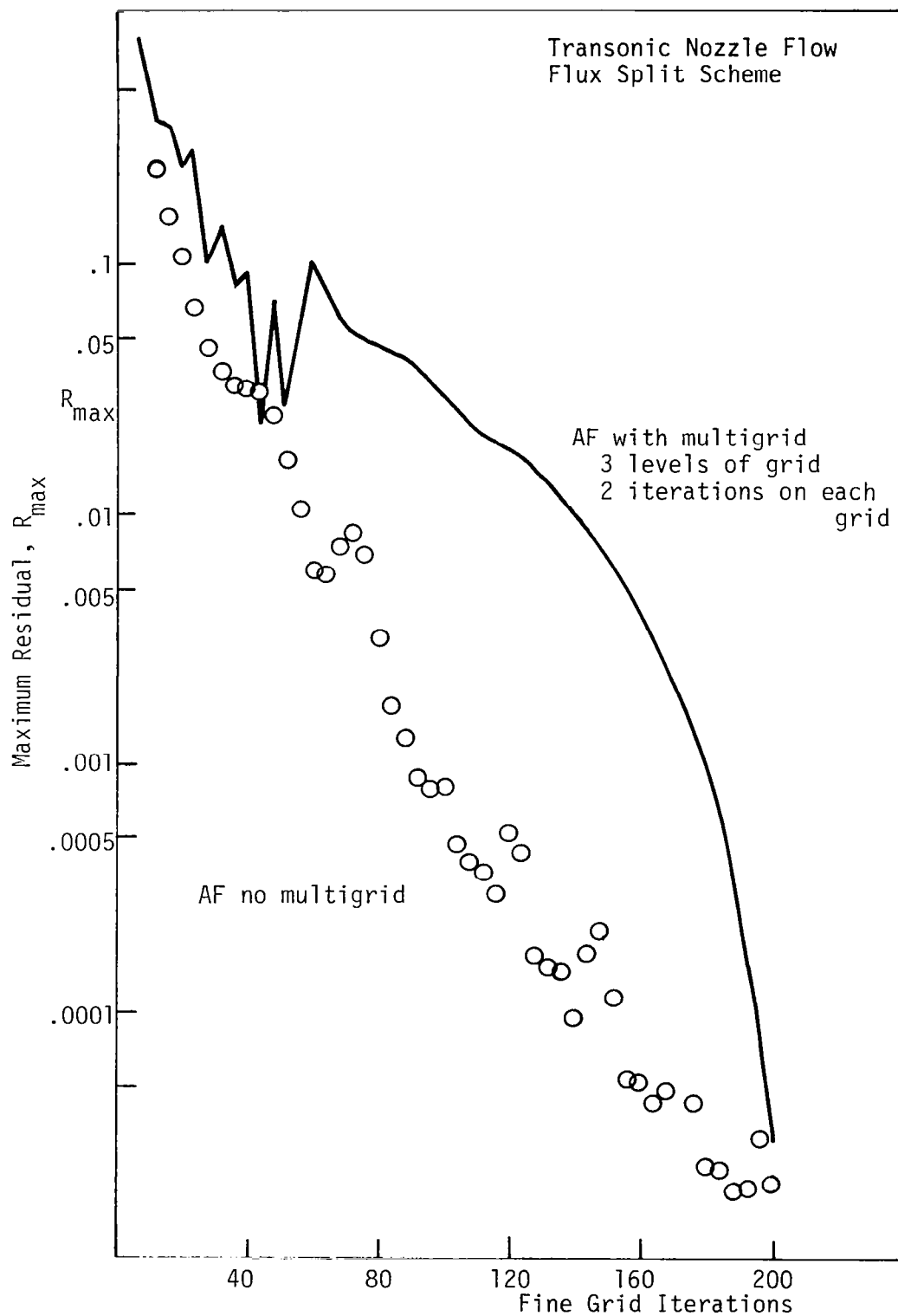


Fig. 3.3. Convergence history.

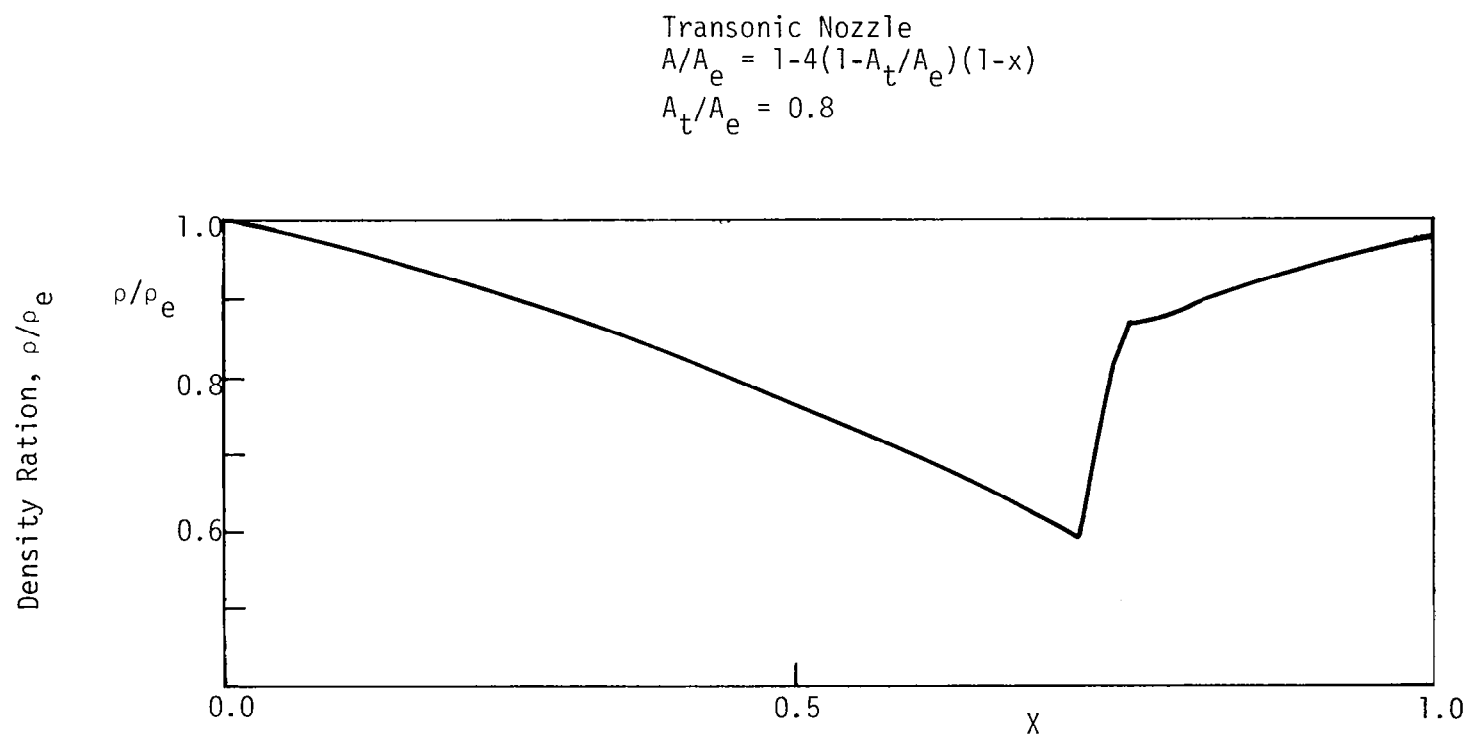


Fig. 3.4. Solution from central differenced algorithm.

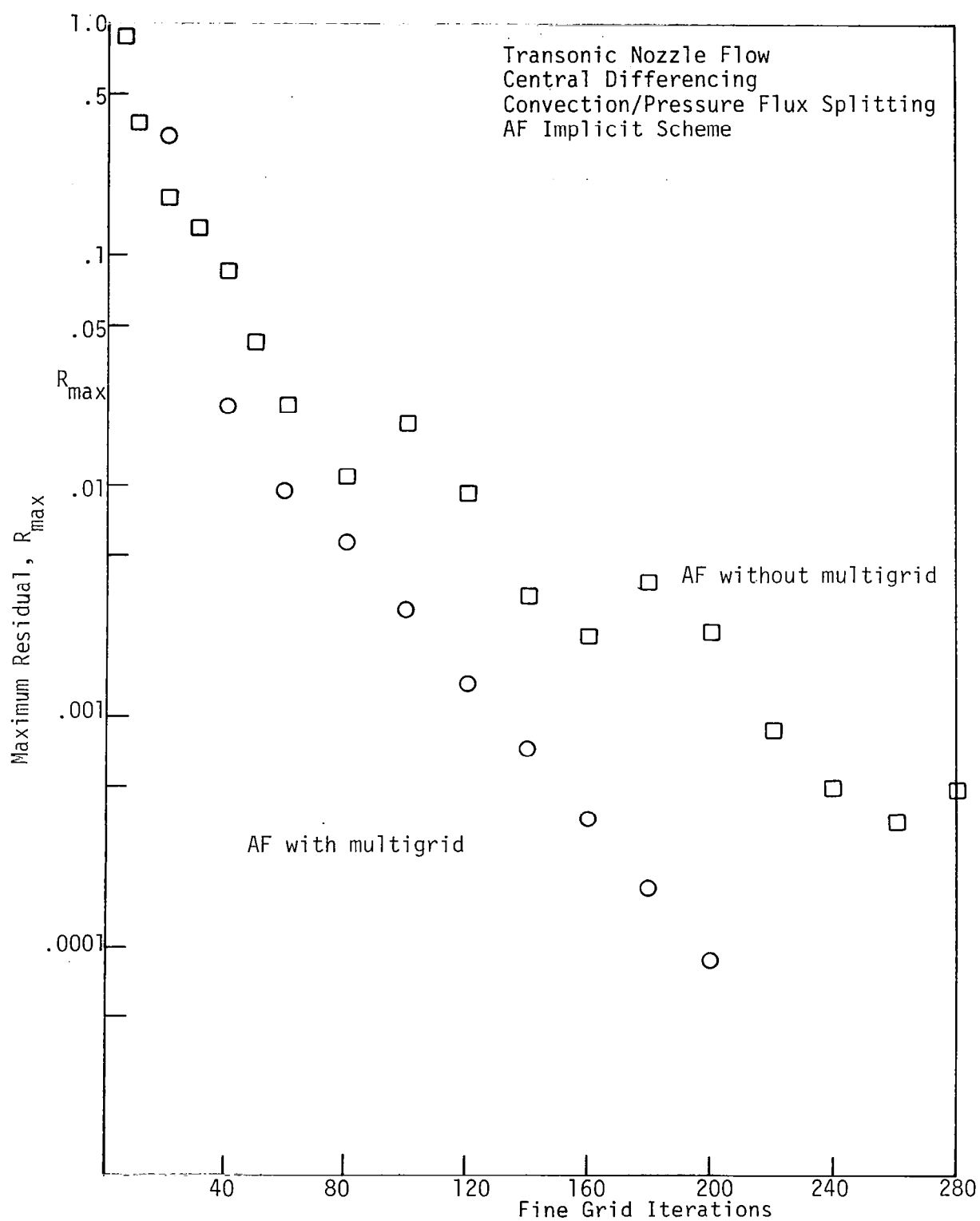


Fig. 3.5. Convergence history.

Biconvex Profile
6 percent thick
 $M_\infty = 0.817$
65 x 33 grid

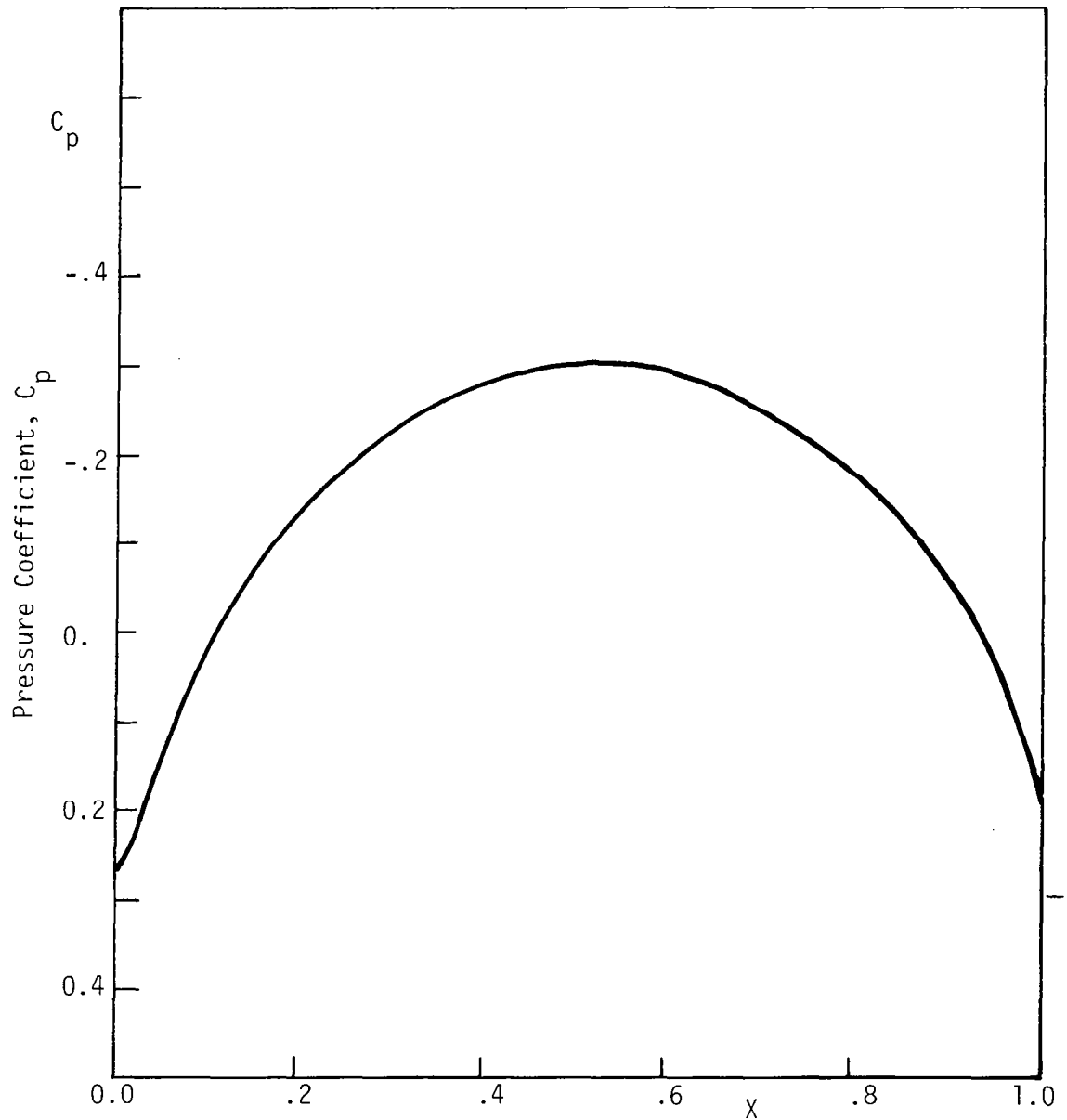


Fig. 4.1. Subcritical solution obtained with plus-minus flux splitting.

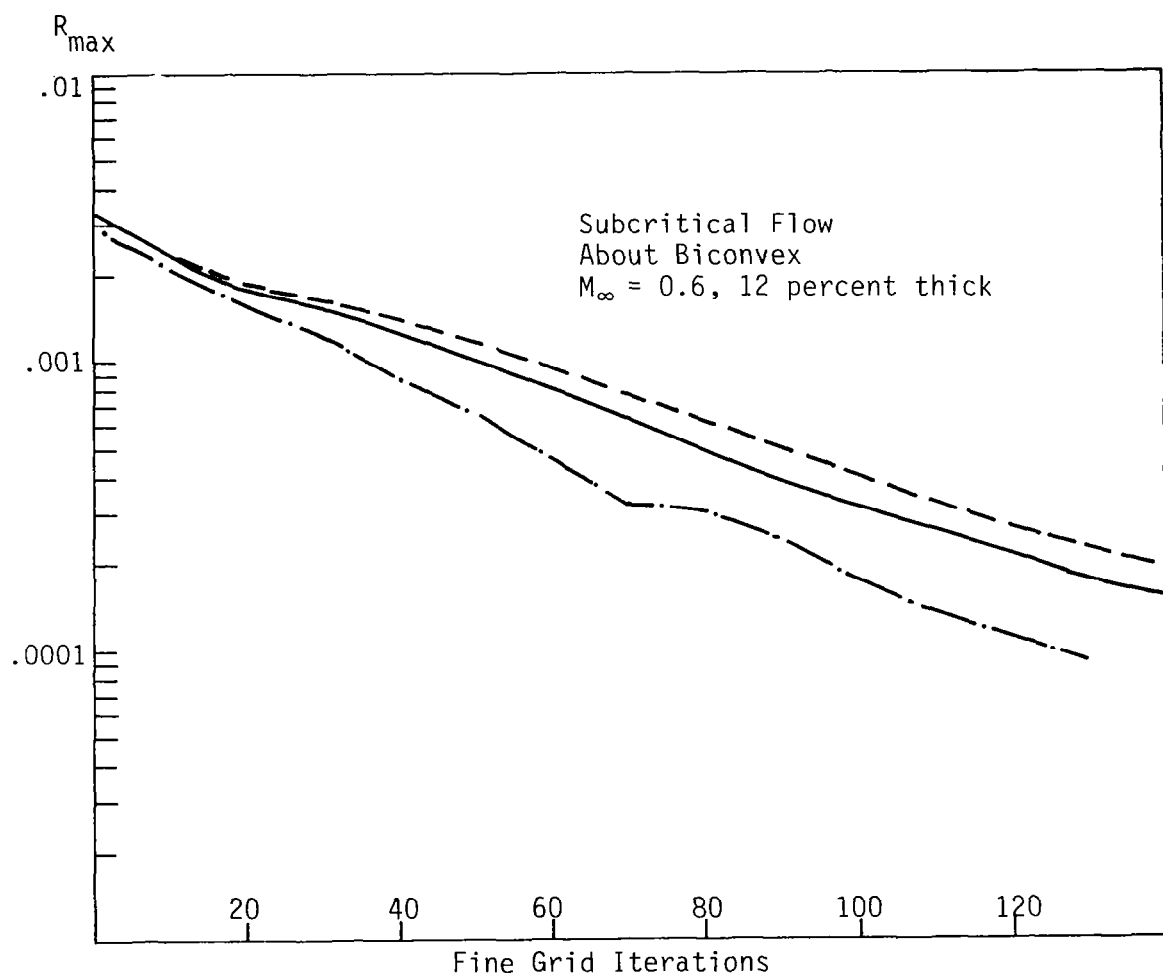


Fig. 4.2. Convergence history of basic algorithm without multigrid.

Plus-Minus Flux Split
Multigrid
Biconvex, 6 percent thick
 $M_\infty = 0.817$

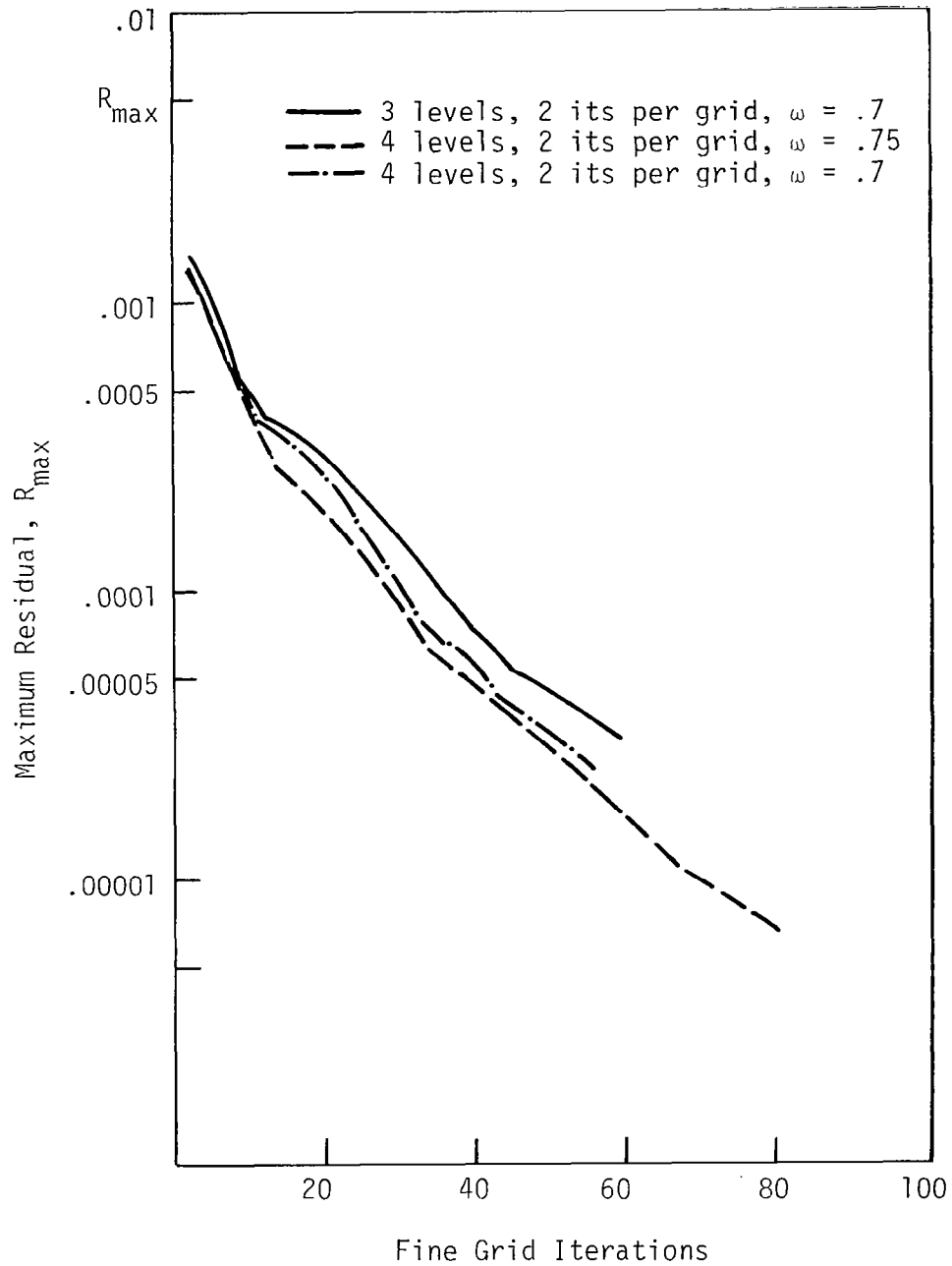


Fig. 4.3. Convergence history of subcritical flow about nonlifting airfoil using multigrid.

Biconvex
 12 percent thick
 $M_\infty = 0.8$
 65 x 33 grid

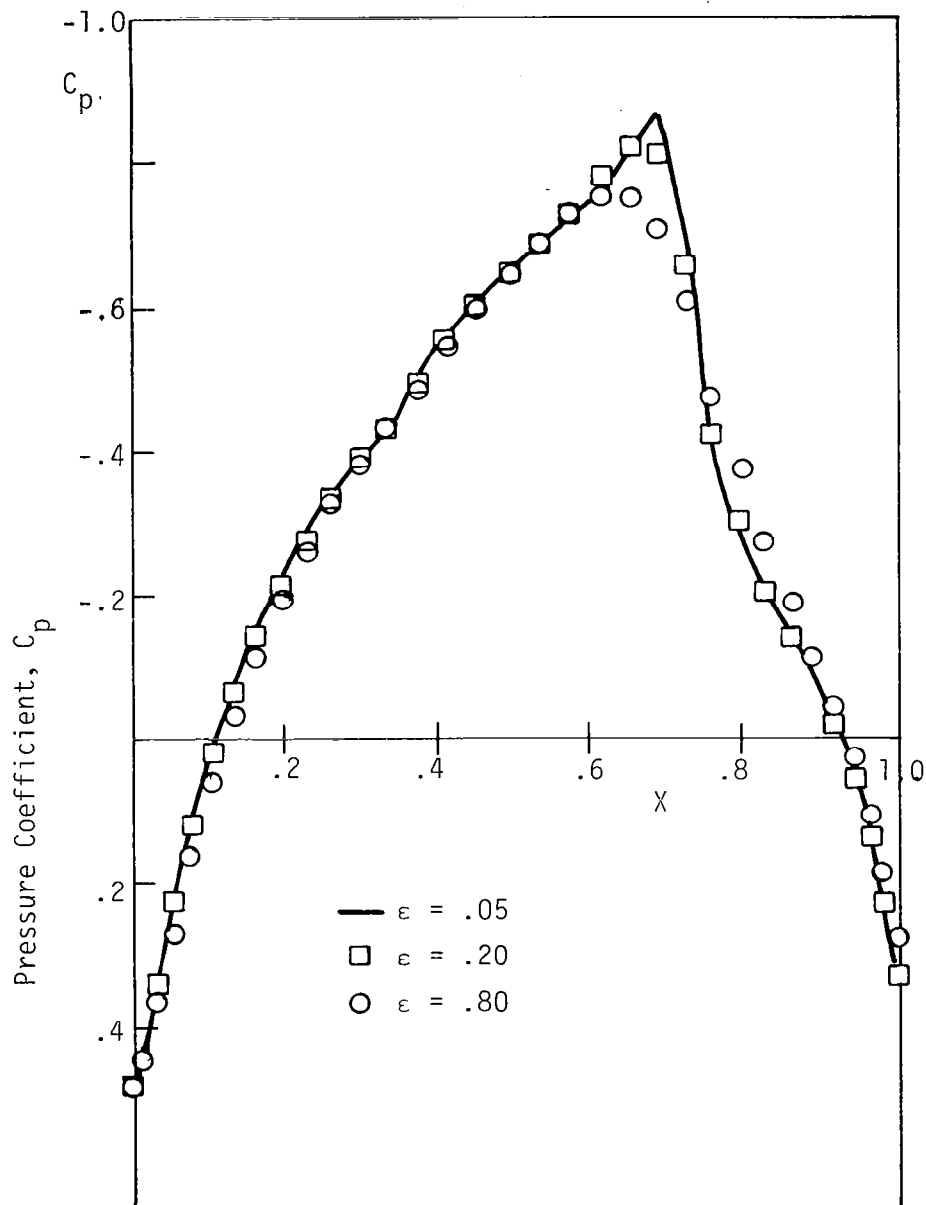


Fig. 4.4. Solution for flow about biconvex using plus-minus flux split scheme.

Transonic Flow
 Biconvex
 12 percent thick
 $M_\infty = 0.80$
 65 x 33 stretched grid
 No multigrid

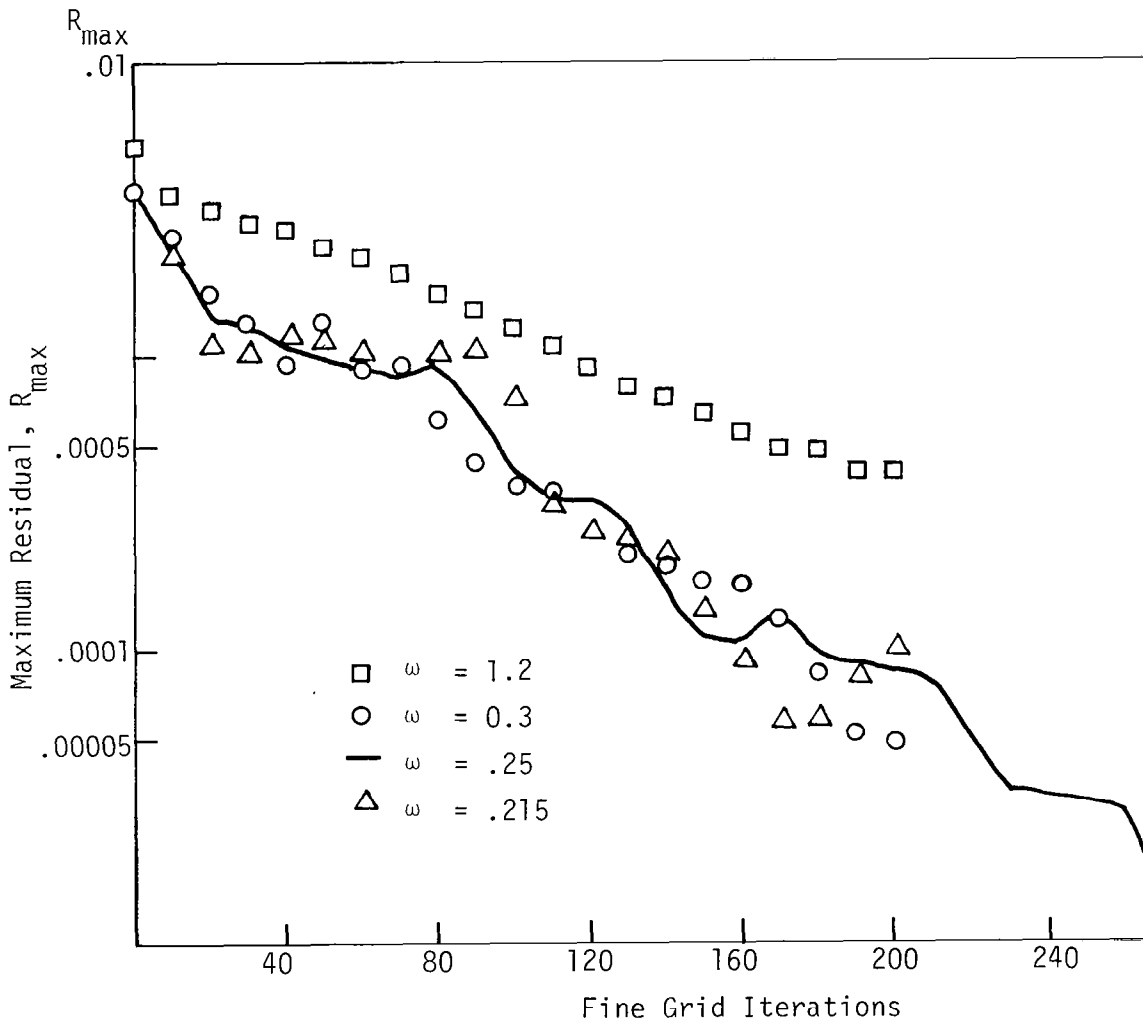


Fig. 4.5. Convergence history of AF implicit scheme without multigrid for various relaxation parameters.

Transonic Flow
Biconvex, $M_\infty = 0.8$
12 percent thick
65 x 33 grid
3 levels, 2 its per grid
 $\omega = 0.165$

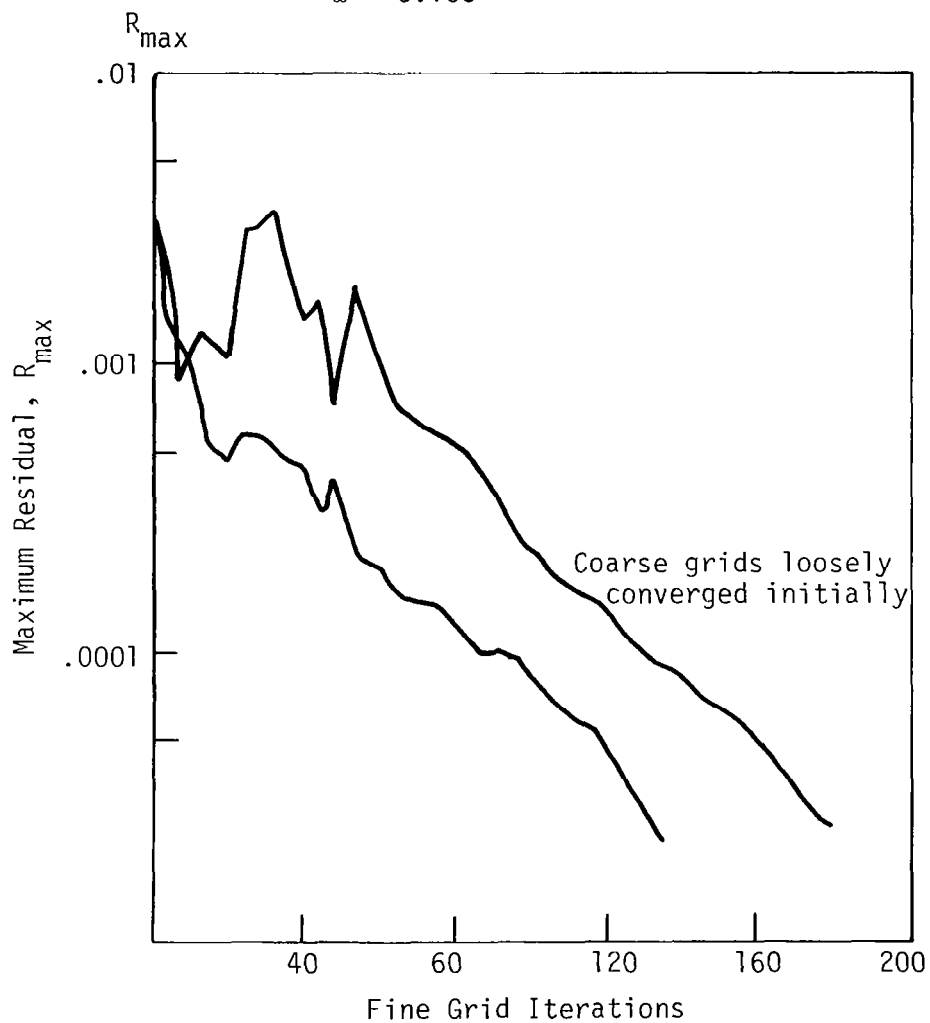
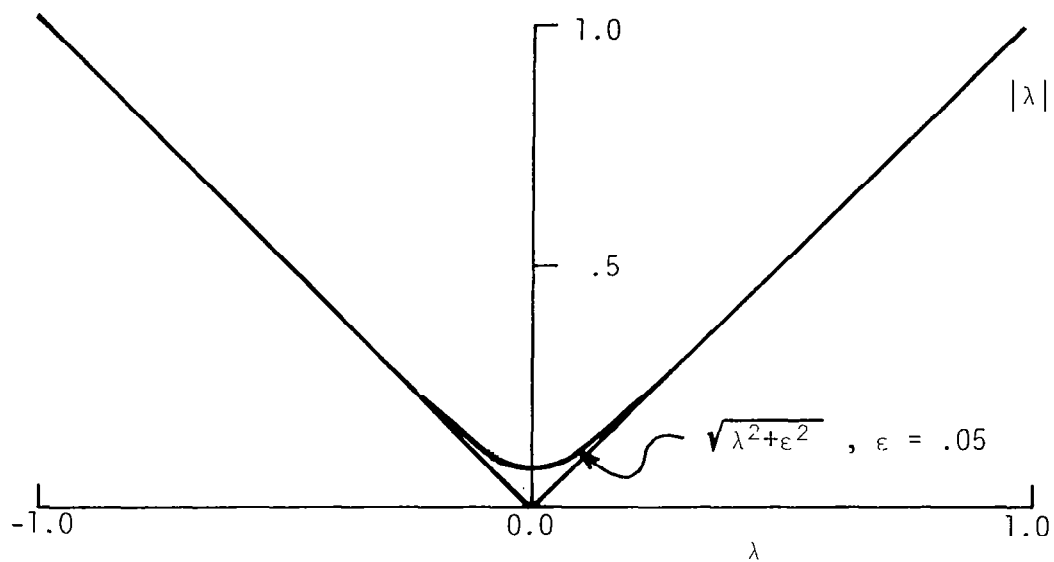


Fig. 4.6. Convergence history using best multigrid.



Hyperbola approximation to $|\lambda|$

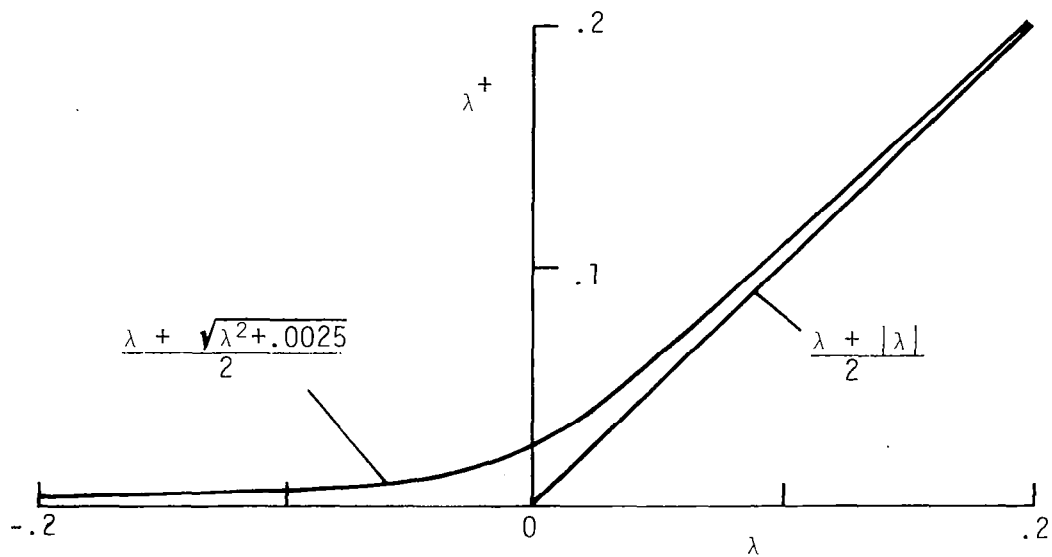


Fig. 5.1. Continuous λ^+ using hyperbola fit.

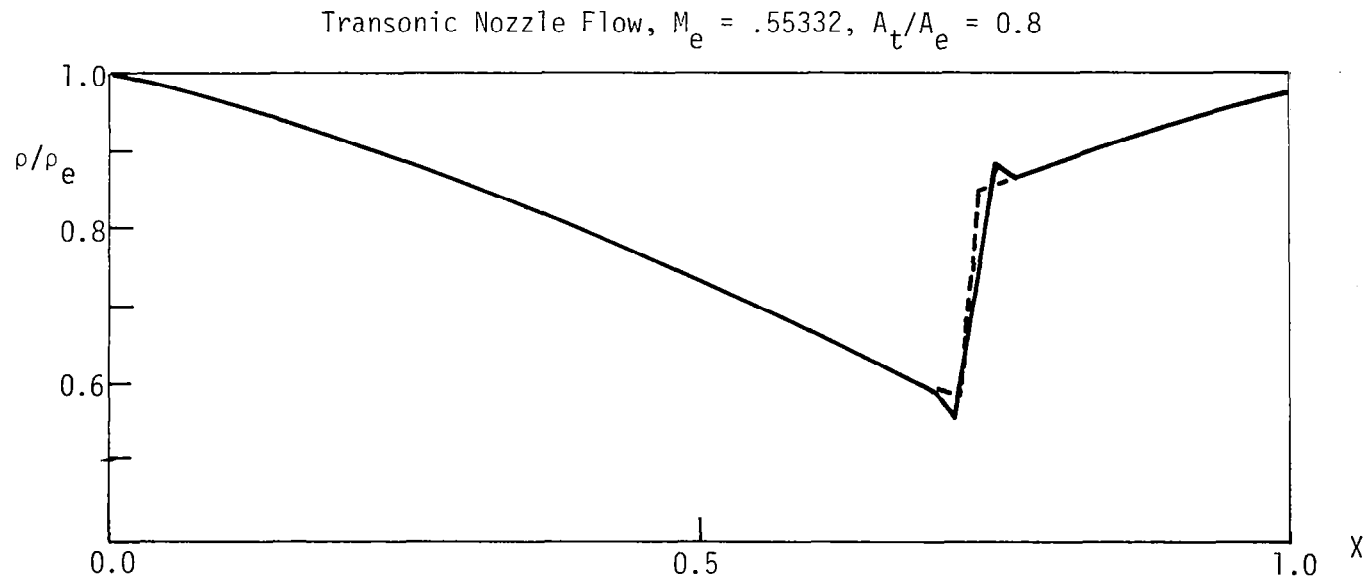


Fig. 5.2. Solutions to one dimensional nozzle using continuous derivative flux splitting - Bram van Leer flux vectors.

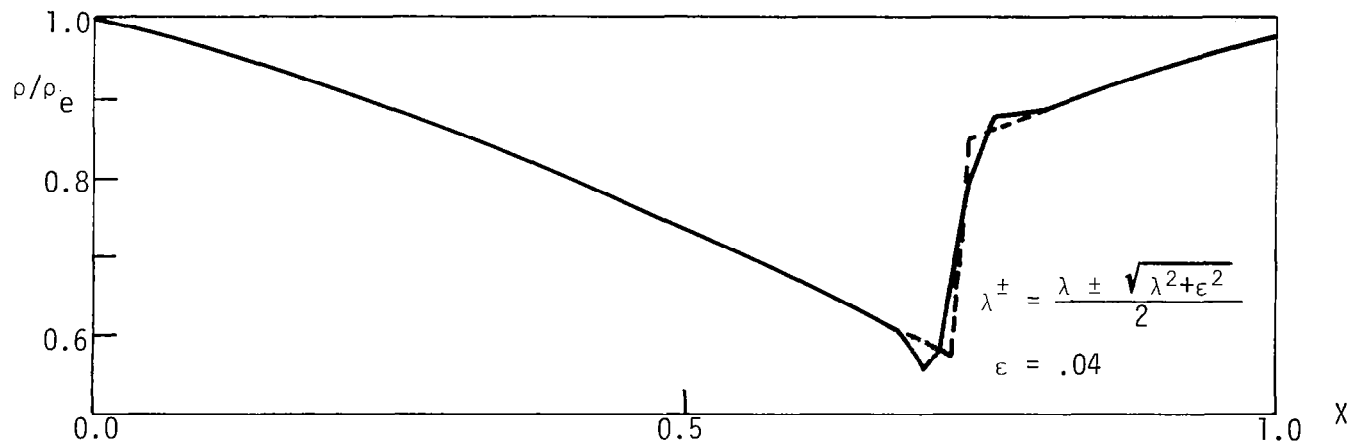


Fig. 5.3. Solutions to one dimensional nozzle using continuous derivative flux splitting - Steger-Warming flux vectors.

APPENDIX A

Multigrid Methodology

Denote the difference equations for the flux split partial differential equation as

$$R(q) = \delta_x^b E^+ + \delta_x^f E + \delta_y^b F^+ + \delta_y^f F^- = 0$$

where

$$E = E(q), \quad F = F(q)$$

Define grids $G_1, G_2, G_3, \dots, G_m, \dots, G_M$ where G_M is the finest grid. As in matrix notation, the higher the value of m , the more elements or points. Let q be a solution to the difference equations, and let \tilde{q} be an approximate solution. Expand $R(q) = 0$ about \tilde{q} , then

$$R(q) = R(\tilde{q}) + A(q - \tilde{q}) + O(q - \tilde{q})^2 \quad (A.1)$$

where $A = \frac{\partial R(\tilde{q})}{\partial \tilde{q}}$ is the Jacobian matrix of the entire set of difference equations.

On the fine grid (A.1) is rewritten

$$A_M(q_M - \tilde{q}_M) = R_M(q) - R_M(\tilde{q}) \equiv R_M - \tilde{R}_M \quad (A.2)$$

where subscript M denotes the finest or M th grid. Let I_M^{M-1} be the averaging operator from M to the grid $M-1$, then (A.2) can be multiplied by I_M^{M-1} to obtain

$$I_M^{M-1} A_M(q_M - \tilde{q}_M) = I_M^{M-1} (R_M - \tilde{R}_M)$$

or approximately

$$I_M^{M-1} A_M I_{M-1}^M I_M^{M-1} (q_M - \tilde{q}_M) \doteq I_M^{M-1} (R_M - \tilde{R}_M) \quad (A.3)$$

where I_{M-1}^M is the interpolation operator from grid M-1 to M.
Note that

$$I_{M-1}^M I_M^{M-1} = I_M^M \quad (A.4)$$

where I_M^M is an approximate identity of rank corresponding with the Mth grid.

To the same approximation one can let

$$I_M^{M-1} A_M I_{M-1}^M \doteq A_{M-1} \equiv \frac{\partial R_{M-1}}{\partial q_{M-1}} \quad (A.5)$$

Although this last step is unnecessary, it is useful for programming ease. With use of (A.5), equation (A.3) is rewritten

$$A_{M-1} I_M^{M-1} (q_M - \tilde{q}_M) = I_M^{M-1} (R_M - \tilde{R}_M) \quad (A.6)$$

which can be represented as

$$Ae = f \quad (A.7)$$

where A = coefficient matrix, e = discrepancy variable,
and f = residual forcing function.

Without making the substitution (A.5), the only required approximation in the reduced system (A.6) or (A.7) is in equation (A.4). Except for this approximation, a solution to the reduced system (A.6) is a solution to (A.2).

Rather than solve (A.6) or (A.7) directly, an iterative solution can be sought of the form

$$e^{n+1} - e^n = H(Ae^n - f) \quad (A.8)$$

where H is the conditioning matrix defined by the iteration scheme.

Once an approximate iterative solution is obtained from (A.6), call it e_{M-1} , the new estimate of $q_M - \tilde{q}_M$ is obtained as

$$q_M - \tilde{q}_M = I_{M-1}^M e_{M-1} \quad (A.9)$$

where

$$e_{M-1} \equiv \bar{A}_{M-1}^{-1} I_M^{M-1} (R_M - \tilde{R}_M)$$

and \bar{A}_{M-1}^{-1} is an iterative approximation to A_{M-1}^{-1} , typically

$$\bar{A}_{M-1}^{-1} = \sum_{n=0}^{n-1} (I + H A_{M-1})^n H \quad (A.10)$$

is the first few terms of the Neumann series. This overall process can be carried out over more than one grid, and with use of various iteration strategies, defines the multigrid technique.

Note that the above discussion doesn't show that this process is efficient or even desirable. It simply defines the mechanics. It seems clear, however, that 1) $I_{M-1}^M I_M^{M-1}$ should approximate I as closely as possible; and

2) that whatever matrix is used to approximate A_{M-1} , it should be as close as $I_M^{M-1} A_M I_M^M$ as possible. Examples of the interpolation matrices follow.

Interpolation Operator I_M^{M+1}

Given data on the odd indexed points, as shown,

$$\begin{array}{ccccccccc} 0 & 0 & 0 & 0 & 0 & 0 & 0 & 0 & 0 \\ 1 & 2 & 3 & 4 & 5 & 6 & 7 & 8 & 9 \end{array}$$

use linear interpolation for even indexed points, that is

$$u_2 = \frac{u_1 + u_3}{2}, \quad u_4 = \frac{u_3 + u_5}{2}, \quad \text{etc.}$$

In matrix form the equations are written for a nine point grid as

$$\begin{bmatrix} u_1 \\ u_2 \\ u_3 \\ u_4 \\ u_5 \\ u_6 \\ u_7 \\ u_8 \\ u_9 \end{bmatrix} = \frac{1}{2} \begin{bmatrix} 2 & & & & & & & & \\ & 1 & 1 & & & & & & \\ & & 2 & & & & & & \\ & & & 1 & 1 & & & & \\ & & & & 2 & & & & \\ & & & & & 1 & 1 & & \\ & & & & & & 2 & & \\ & & & & & & & 1 & 1 \\ & & & & & & & & 2 \end{bmatrix} \begin{bmatrix} u_1 \\ u_3 \\ u_5 \\ u_7 \\ u_9 \end{bmatrix} = \begin{bmatrix} u_1 \\ (u_2+u_3)/2 \\ u_3 \\ (u_3+u_5)/2 \\ u_5 \\ (u_5+u_7)/2 \\ u_7 \\ (u_7+u_9)/2 \\ u_9 \end{bmatrix}$$

In the multigrid notation the equations are represented as

$$u_{m+1} = I_m^{m+1} u_m$$

Use of other than linear interpolation defines a new matrix I_m^{m+1} .

Averaging Operator I_{m+1}^m

Given data at all grid points,

$$\begin{array}{ccccccccc} 0 & 0 & 0 & 0 & 0 & 0 & 0 & 0 & 0 \\ 1 & 2 & 3 & 4 & 5 & 6 & 7 & 8 & 9 \end{array}$$

average the data for the interior odd-indexed points,
that is

$$\begin{aligned} u_3 &= \frac{u_2 + 2u_3 + u_5}{4} \\ u_5 &= \frac{u_4 + 2u_5 + u_6}{4}, \text{ etc.} \end{aligned}$$

In matrix form the equations are written for a nine point grid

$$\begin{bmatrix} u_1 \\ u_3 \\ u_5 \\ u_7 \\ u_9 \end{bmatrix} = \frac{1}{4} \begin{bmatrix} 4 & & & & \\ & 1 & 2 & 1 & \\ & & & 1 & 2 & 1 \\ & & & & & 1 & 2 & 1 \\ & & & & & & & 4 \end{bmatrix} \begin{bmatrix} u_1 \\ u_2 \\ u_3 \\ u_4 \\ u_5 \\ u_6 \\ u_7 \\ u_8 \\ u_9 \end{bmatrix} = \begin{bmatrix} u_1 \\ (u_2+2u_3+u_4)/4 \\ (u_4+2u_5+u_6)/4 \\ (u_6+2u_7+u_8)/4 \\ u_9 \end{bmatrix}$$

In the multigrid notation the equations are represented
as

$$u_m = I_{m+1}^m u_{m+1}$$

If injection is used the matrix I_{m+1}^m has the form for the 5×9

$$I_{m+1}^m = \begin{bmatrix} 1 & 0 & & & & & & & \\ & 0 & 1 & 0 & & & & & \\ & & & 0 & 1 & 0 & & & \\ & & & & 0 & 1 & 0 & & \\ & & & & & 0 & 1 & 0 & \\ & & & & & & 0 & 1 & \end{bmatrix}$$

Approximate Reduced Identity

$$I_m^{m-1} I_{m-1}^m = I_{m-1}^{m-1}$$

$$\frac{1}{4} \begin{bmatrix} 4 & & & & & & & & \\ & 1 & 2 & 1 & & & & & \\ & & 1 & 2 & 1 & & & & \\ & & & 1 & 2 & 1 & & & \\ & & & & 1 & 2 & 1 & & \\ & & & & & & 4 & & \end{bmatrix} \frac{1}{2} \begin{bmatrix} 2 & & & & & & & & \\ 1 & 1 & & & & & & & \\ & 2 & & & & & & & \\ & & 1 & 1 & & & & & \\ & & & 2 & & & & & \\ & & & & 1 & 1 & & & \\ & & & & & 2 & & & \\ & & & & & & 1 & 1 & \\ & & & & & & & 2 & \end{bmatrix} = \frac{1}{8} \begin{bmatrix} 8 & 0 & 0 & 0 & 0 \\ 1 & 6 & 1 & 0 & 0 \\ 0 & 1 & 6 & 1 & 0 \\ 0 & 0 & 1 & 6 & 1 \\ 0 & 0 & 0 & 0 & 8 \end{bmatrix}$$

$$= I + \frac{1}{8} \begin{bmatrix} \circ & & & & \\ \nabla \Delta & \cdot & & & \\ & \cdot & \cdot & & \\ & & \cdot & \cdot & \\ & & & \nabla \Delta & \circ \end{bmatrix}$$

Approximate Expanded Identity

$$I_{m-1}^m I_m^{m-1} = I_m^m$$

$$\frac{1}{8} \begin{bmatrix} 2 & & & & & & \\ 1 & 1 & & & & & \\ & 2 & & & & & \\ & & 1 & 1 & & & \\ & & & 2 & & & \\ & & & & 1 & 1 & \\ & & & & & 2 & \\ & & & & & & 1 & 1 \\ & & & & & & & 2 \end{bmatrix} \begin{bmatrix} 4 & & & & & & \\ & 1 & 2 & 1 & & & \\ & & & 1 & 2 & 1 & \\ & & & & & 1 & 2 & 1 \\ & & & & & & & 4 \end{bmatrix} = \frac{1}{8} \begin{bmatrix} 8 & & & & & & \\ 4 & 1 & 2 & 1 & & & \\ & 2 & 4 & 2 & & & \\ & & 1 & 2 & 2 & 2 & 1 \\ & & & 2 & 4 & 2 & \\ & & & & 1 & 2 & 2 & 2 & 1 \\ & & & & & 2 & 4 & 2 \\ & & & & & & 1 & 2 & 1 & 4 \\ & & & & & & & & & 8 \end{bmatrix}$$

APPENDIX B

The relation of the upwind plus-minus split scheme to central differencing schemes is reviewed here following unpublished work of Ami Harten. We previously defined

$$A^+ = S \left(\frac{\Lambda + |\Lambda|}{2} \right) S^{-1} , \quad A^{-1} = S \left(\frac{\Lambda - |\Lambda|}{2} \right) S^{-1}$$

so

$$\begin{aligned} A^+ &= \frac{S \Lambda S^{-1}}{2} + \frac{S |\Lambda| S^{-1}}{2} \\ &\equiv (A + |A|)/2 , \quad F^+ = (F + |A|q)/2 \end{aligned} \quad (B.1a)$$

and

$$A^- = (A - |A|)/2 , \quad F^- = (F - |A|q)/2 \quad (B.1b)$$

Apply these into our equation (8.4) of TM 78605
(reference [1])

$$\begin{aligned} &\left[I + \frac{\theta \Delta t}{1 + \xi} (\nabla_x A_{j,k}^+ |^n + \Delta_x A_{j,k}^- |^n + \nabla_y B_{j,k}^+ |^n + \Delta_y B_{j,k}^- |^n) \right] \Delta q_{j,k}^n \\ &= - \left(\frac{\Delta t}{1 + \xi} \right) (\delta_{x F_{j,k}}^{b+} |^n + \delta_{x F_{j,k}}^{f-} |^n + \delta_{y G_{j,k}}^{b+} |^n + \delta_{y G_{j,k}}^{f-} |^n) \\ &\quad + \left(\frac{\xi}{1 + \xi} \right) \Delta q_{j,k}^{n-1} \end{aligned} \quad (B.2)$$

giving (pull $\frac{1}{2}$ out in front)

$$\begin{aligned}
 & \left[I + \frac{1}{2} \frac{\theta \Delta t}{(1+\xi)} \{ (\nabla_{\mathbf{x}} + \Delta_{\mathbf{x}}) A^n + \nabla_{\mathbf{x}} |A| - \Delta_{\mathbf{x}} |A| + (\nabla_{\mathbf{y}} + \Delta_{\mathbf{y}}) B^n \right. \\
 & \quad \left. + \nabla_{\mathbf{y}} |B| - \Delta_{\mathbf{y}} |B| \} \right] \Delta q^n = -\frac{1}{2} \left(\frac{\Delta t}{1+\xi} \right) (\delta_{\mathbf{x}}^b (F + |A|q) \\
 & \quad + \delta_{\mathbf{y}}^b (F - |A|q) + \delta_{\mathbf{y}}^b (G + |B|q) + \delta_{\mathbf{y}}^f (G - |B|q))^n + \frac{\xi}{1+\xi} \Delta q^{n-1}
 \end{aligned} \tag{B.3}$$

Define the centered difference operators

$$\frac{\nabla_{\mathbf{x}} + \Delta_{\mathbf{x}}}{2} = \frac{E - E^{-1}}{2\Delta x} = \delta_{\mathbf{x}} \tag{B.4a}$$

$$\nabla_{\mathbf{x}} - \Delta_{\mathbf{x}} = \frac{-E^{+1} + 2I - E^{-1}}{\Delta x} = -(\Delta x)^{-1} (\nabla) \tag{B.4b}$$

$$\frac{\delta_{\mathbf{x}}^b + \delta_{\mathbf{x}}^f}{2} = \frac{+E^{-2} - 4E^{-1} + 4E - E^{+2}}{4\Delta x} \bar{\delta}_{\mathbf{x}} \tag{B.4c}$$

$$\delta_{\mathbf{x}}^b - \delta_{\mathbf{x}}^f = \frac{E^{-1} - 4E^{-1} + 6 - 4E + E^{+2}}{2\Delta x} \equiv (2\Delta x)^{-1} (\nabla)^2 \tag{B.4d}$$

and substitute these into (B.3)

$$\begin{aligned}
 & \left[I + \left(\frac{\theta \Delta t}{1+\xi} \right) (\delta_{\mathbf{x}} A^n + \delta_{\mathbf{y}} B^n - (2\Delta x)^{-1} (\nabla) |A| - (2\Delta y)^{-1} (\nabla) |B|) \right] \Delta q^n \\
 & = -\left(\frac{\Delta t}{1+\xi} \right) (\bar{\delta}_{\mathbf{x}} F^n + \bar{\delta}_{\mathbf{y}} G^n + (4\Delta x)^{-1} (\nabla)^2 |A| q^n + (4\Delta y)^{-1} (\nabla)^2 |B| q^n) \\
 & + \frac{\xi}{1+\xi} \Delta q^{n-1}
 \end{aligned} \tag{B.5}$$

Equation (B.5) represents a conventional central difference scheme with second and fourth order dissipation terms. Further simplification is possible.

Define the spectral radius $\rho = |\lambda_{\max}|$ and replace $|A|$ with ρ_a , $|B|$ with ρ_b . Then (B.5) is approximated as

$$\begin{aligned} & \left[I + \frac{\theta \Delta t}{(1+\xi)} (\delta_x A^n + \delta_y B^n - \frac{\nabla \Delta \rho_a}{2\Delta x} - \frac{\nabla \Delta \rho_b}{2\Delta y}) \right] \Delta q^n \\ & - \left(\frac{\Delta t}{1+\xi} \right) (\bar{\delta}_x F^n + \bar{\delta}_y G^n + \frac{(\nabla \Delta)^2 \rho_a}{4\Delta x} + \frac{(\nabla \Delta)^2 \rho_b}{4\Delta y} q^n) + \left(\frac{\xi}{1+\xi} \right) \Delta q^{n-1} \end{aligned} \quad (B.6)$$

or in factored form

$$\begin{aligned} & \left[I + \frac{\theta \Delta t}{(1+\xi)} (\delta_x A^n - \frac{\nabla \Delta \rho_a}{2\Delta x}) \right] \left[I + \frac{\theta \Delta t}{(1+\xi)} (\delta_y B^n - \frac{\nabla \Delta \rho_b}{2\Delta y}) \right] \Delta q^n \\ & = \text{RHS (B.6)} \end{aligned} \quad (B.7)$$

Equation (B.7) has the same type of numerical dissipation terms used in our conventional central difference scheme (c.f. Steger and Baily, AIAA J., March, 1980).

The left-hand side of the scheme (B.2) can be factored into the product of two operators as

$$\begin{aligned} & \left[I + h(\nabla_x A_{j,k}^+ |^n + \nabla_y B_{j,k}^+ |^n) \right] \left[I + h(\Delta_x A_{j,k}^- |^n \right. \\ & \left. + \Delta_y B_{j,k}^- |^n) \right] \Delta q^n = \text{RHS (B.2)} \end{aligned} \quad (B.8)$$

where

$$h = \frac{\theta \Delta t}{1 + \xi}$$

Substitution of (B.1) into the above

$$\begin{aligned} & \left[I + h(\nabla_x(\frac{A+|A|}{2}) + \nabla_y(\frac{B+|B|}{2})) \right] \left[I + h(\Delta_x(\frac{A-|A|}{2}) + \Delta_y(\frac{B-|B|}{2})) \right] \Delta q^n \\ & = \text{RHS (B.3)} \end{aligned}$$

Replace $|A| = \rho_a I$ and $|B| = \rho_b I$ which degrades the time accuracy to $O(\Delta t)$. Then

$$\begin{aligned} & \left[I + h\nabla_x \frac{(\rho_a I + A)}{2} + \frac{h\nabla_y(\rho_b I + B)}{2} \right] \left[I + \frac{h\Delta_x(A - \rho_a I)}{2} \right. \\ & \quad \left. + h\Delta_y \frac{(B - \rho_b I)}{2} \right] \Delta q^n = \text{RHS (B.6)} \end{aligned}$$

APPENDIX C

Using a "Lax-Wendroff trick" one can write the Euler equations as a second order wave-equation. This leads to a time accurate formulation which for steady state problems is a particular case of Johnson's surrogate equation approach.

The Euler equations are differentiated in time

$$\partial_t(\partial_t q + \partial_x E + \partial_y F) = 0 \quad (C.1)$$

giving

$$(\partial_t + \partial_x A + \partial_y B) \partial_t q = 0 \quad (C.2)$$

as $\partial_t \partial_x E = \partial_x \partial_t E = \partial_x E q_t = \partial_x A q_t$, etc.

But $\partial_t q = -\partial_x E + \partial_t F$ so (C.2) is rewritten as
(a similar substitute is used in the Lax Wendroff scheme)

$$\partial_{tt} q = (\partial_x A + \partial_y B)(\partial_x E + \partial_y F) \quad (C.3)$$

Expanding (C.3) gives the desired form

$$\partial_{tt} q = \partial_x A \partial_x E + \partial_x A \partial_y F + \partial_t B \partial_x E + \partial_y B \partial_y F \quad (C.4)$$

or making use of the fact that the equations are homogeneous of degree one

$$(\partial_{tt} - \partial_x A \partial_x A - \partial_x A \partial_y B - \partial_y B \partial_x A - \partial_y B \partial_y B) q = 0 \quad (C.5)$$

The last form (C.5) shows the structure of the equation while the right hand side of (C.3) gives a particular case of Johnson's surrogate equation approach.

1. Report No. NASA CR-3415		2. Government Accession No.		3. Recipient's Catalog No.	
4. Title and Subtitle A PRELIMINARY STUDY OF RELAXATION METHODS FOR THE INVISCID CONSERVATIVE GASDYNAMICS EQUATIONS USING FLUX SPLITTING				5. Report Date March 1981	
				6. Performing Organization Code	
7. Author(s) Joseph L. Steger				8. Performing Organization Report No. FSI 80-4	
				10. Work Unit No.	
9. Performing Organization Name and Address Flow Simulations, Inc. 298 S. Sunnyvale Ave., Suite 204 Sunnyvale, California 94086				11. Contract or Grant No. NAS1-15852	
				13. Type of Report and Period Covered Contractor report	
12. Sponsoring Agency Name and Address National Aeronautics and Space Administration Washington, D.C. 20546				14. Sponsoring Agency Code	
15. Supplementary Notes Langley Technical Monitor: Stephen F. Wornom Final Report					
16. Abstract <p>The purpose of this study was to combine recently introduced plus-minus flux vector split schemes with the multigrid relaxation method to obtain fast rates of iterative (or steady state) convergence. On model nonlifting biconvex airfoil flow, steady state convergence has been obtained using multigrid in 40 iterations for subsonic cases and in 120 iterations for transonic cases. A 65×33 stretched grid was used. However, the multigrid scheme used here (and there are numerous variations) sometimes could not be made to work for transonic cases with a large number of supersonic points. Moreover, the multigrid method was only several times faster than the conventional algorithm which itself could perhaps be accelerated by other means. Nevertheless one quickly becomes convinced that with proper adjustment the multigrid method will ultimately lead to very fast rates of iterative convergence.</p>					
17. Key Words (Suggested by Author(s)) Relaxation Methods Gasdynamics Flux Splitting Multigrid			18. Distribution Statement Unclassified - Unlimited Subject Category 64		
19. Security Classif. (of this report) Unclassified	20. Security Classif. (of this page) Unclassified	21. No. of Pages 53	22. Price A04		